

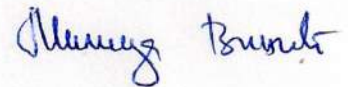
Научном већу Института за физику

Предмет: Молба за покретање поступка за реизбор у звање истраживач сарадник

У складу са критеријумима прописаним од стране Министарства за просвету, науку и технолошки развој за стицање истраживачког звања истраживач сарадник, као и критеријуме прописане од стране Правилника о поступку и начину вредновања, и квантитативном исказивању научно-истраживачких резултата истраживача, молим научно веће Института за физику да покрене поступак за мој реизбор у звање истраживач сарадник.

18. октобар 2018.
Београд

С поштовањем,
Милица Винић



Научном већу Института за физику

Предмет: Мишљење руководиоца пројекта за реизбор Милице Виноћ у звање истраживач сарадник

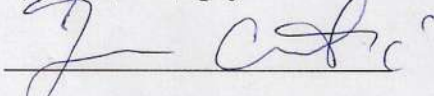
Милица Виноћ, запослена у Лабораторији за спектроскопију плазме и физику ласера Института за физику, ангажована је на пројектима: (1) из области основних истраживања ОИ171014 под насловом „Спектроскопска дијагностика нискотемпературне плазме и гасних пражњења: облици спектралних линија и интеракција са површинама“; (2) из области технолошког развоја ТР 37019 „Електродинамика атмосфере у урбаним срединама Србије“. Оба пројекта финансира Министарство просвете, науке и технолошког развоја Републике Србије. На поменутиим пројектима ради на теми ласерске аблације.

С обзиром да испуњава све предвиђене услове, у складу са Законом о научно-истраживачкој делатности за изборе у истраживачка звања, сагласни смо са покретањем поступка за реизбор Милице Виноћ у звање истраживач сарадник.

За чланове Комисије за реизбор Милице Виноћ у звање истраживач сарадник предлажемо:

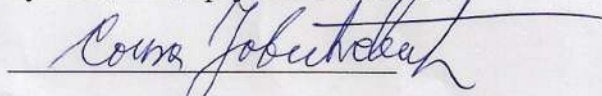
1. др Миливоје Ивковић, научни саветник, Институт за физику
2. др Маријана Гавриловић Божовић, научни сарадник, Институт за физику
3. др Мирослав Кузмановић, ванредни професор, Факултет за Физичку хемију

Руководилац пројекта ТР 37019

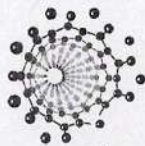


др Јован Цветић, редовни професор,
Електротехнички факултет

Руководилац пројекта ОИ 171014



др Соња Јовићевић
научни саветник, Институт за физику



Република Србија
Универзитет у Београду
Факултет за физичку хемију
Д.Бр.2013/0304
Датум: 16.10.2018. године

На основу члана 29. Закона о општем управном поступку ("Сл. гласник РС", бр.18/2016) и службене евиденције издаје се

УВЕРЕЊЕ

Винић (Весна) Милица, бр. индекса 2013/0304, рођена 12.03.1989. године, Чачак, Чачак-град, Република Србија, уписана школске 2018/2019. године, у статусу: самофинансирање; тип студија: докторске академске студије; студијски програм: Физичка хемија.

Према Статуту факултета студије трају (број година): три године.
Рок за завршетак студија: у двоструком трајању студија.

Ово се уверење може употребити за регулисање војне обавезе, издавање визе, права на дечији додатак, породичне пензије, инвалидског додатка, добијања здравствене књижице, легитимације за повлашћену возњу и стипендије.



Овлашћено лице факултета

[Handwritten signature]

Lični podaci

Ime i prezime: Milica Vinić
Datum rođenja: 12.3.1989.
Adresa: Zemunska 271, Ugrinovci
E – mail: mvinic@ipb.ac.rs
Mobilni: 062/1-43-99-43
Državljanstvo: srpsko



Radno iskustvo

- 12.2015. Istraživač saradnik u Laboratoriji za spektroskopiju plazme i fiziku lasera, Institut za fiziku, Beograd
- 12.2014. Istraživač pripravnik u Laboratoriji za spektroskopiju plazme i fiziku lasera, Institut za fiziku, Beograd

Obrazovanje

- 2013- Upis na doktorske studije
Fakultet za fizičku hemiju, Univerzitet u Beogradu
- 2013 Master fizikohemičar
Fakultet za fizičku hemiju, Univerzitet u Beogradu
Tema master rada: Mogućnosti primene spektroskopije laserom indukovano proboja, za analizu zemljišta
- 2012 Diplomirani fizikohemičar
Fakultet za fizičku hemiju, Univerzitet u Beogradu
Tema diplomskog rada: Ispitivanje laserom indukovane plazme u atmosferi argona

Naučni radovi

- 2018 B. D. Stankov, M. Ivković, M. Vinić and N. Konjević, *Forbidden component of the Be II 436.1nm line recorded from pulsed gas discharge plasma*, EPL 123, 63001
- 2018 B. D. Stankov, M. Vinić, M. R. Gavrilović Božović, and M. Ivković, *Novel plasma source for safe beryllium spectral line studies in the presence of beryllium dust*, Review of Scientific Instruments 89, 053108
- 2014 Vinić Milica, Milivoje Ivković, *Spatial and temporal characteristic of laser ablation combined with fast pulse discharge*, IEEE transactions on plasma science 42, 2598
- 2013 Vinić Milica L., Ivković Milivoje R., *Laser ablation initiated fast discharge for spectrochemical applications*, Hemijska industrija 68, 65

Saopštenja na kongresima

- 2018 M. Vinić, M.R. Gavrilović Božović, B. Stankov, M. Vlanić and M. Ivković, *Nanoparticles on a sample surface as laser induced breakdown spectroscopy enhancers*, 29th Summer School and International Symposium on the Physics of Ionized Gases, Beograd, Srbija, 28. avgust - 1.septembar, str. 190-193
- 2016 M. Vinic, B. Stankov, M. Ivkovic and N. Konjevic, *Characterization of an Atmospheric Pressure Pulsed Microjet*, 28th Summer School and International Symposium on the Physics of Ionized Gases, Beograd, Srbija, 29. avgust - 2.septembar, str. 276
- 2016 M. Vinic, B. Stankov, *Spatial and temporal resolved study of some atmospheric pressure discharges*, Internacionalna konferencija studenata fizike (ICPS), Msida, Malta, 11.-17. avgust, str. 64-65
- 2013 Vinić M., Ivković M., *Klasifikacija zemljišta primenom spektroskopije laserom indukovanoj probolj*, Zbornik radova XII Kongresa fizičara Srbije, 28. april – 2. maj 2013. Vrnjačka Banja, str. 404-407
- 2013 M. Vinic, M. Cvejic and M. Ivkovic, *Spatial and temporal characterisation of combined laser induced plasma and spark technique*, Book of Abstracts 7th Euro-Mediterranean Symposium on Laser Induced Breakdown Spectroscopy, EMSLIBS 2013 Bari (Italija), 16.-20. septembar, 2013, str. 151
- 2012 Vinic M., Ivkovic M. *The emission enhancement in single pulse laser induced breakdown spectroscopy*, Proceedings of the 11th International Conference on Fundamental and Applied Aspects of Physical Chemistry, September 24-26, Beograd, Srbija, str. 134-136

Nagrade i priznanja

- 2014 Nagrada "Pavle Savić", Društvo fizikohemičara Srbije
- 2013 Nagrada za izuzetan uspeh tokom studiranja, Srpsko hemijsko društvo

Lične veštine

- Jezik: Engleski, nivo B2
- Rad na računaru: MS office, Origin
- Vozačka dozvola: B kategorija

Spisak objavljenih radova

Radovi u časopisima

- B. D. Stankov, M. Ivković, M. Vinić and N. Konjević, *Forbidden component of the Be II 436.1nm line recorded from pulsed gas discharge plasma*, EPL 123, 63001, 2018 - M21
- B. D. Stankov, M. Vinić, M. R. Gavrilović Božović, and M. Ivković, *Novel plasma source for safe beryllium spectral line studies in the presence of beryllium dust*, Review of Scientific Instruments 89, 053108, 2018 - M22
- Vinić Milica L, Ivković Milivoje R, *Laser ablation initiated fast discharge for spectrochemical applications*, Hemijska industrija, Volume 68 (3), 381-388, 2014 – M23
- Vinic Milica, Milivoje Ivkovic, *Spatial and temporal characteristic of laser ablation combined with fast pulse discharge*, IEEE transactions on plasma science, Volume 42 (10), p. 2598-2599, 2014 - M23

Radovi na međunarodnim konferencijama štampani u celini M33

- M. Vinić, M.R. Gavrilović Božović, B. Stankov, M. Vlanić and M. Ivković, *Nanoparticles on a sample surface as laser induced breakdown spectroscopy enhancers*, 29th Summer School and International Symposium on the Physics of Ionized Gases, Beograd, Srbija, 28. avgust - 1.septembar 2018, str. 190-193
- M. Vinic, B. Stankov, M. Ivkovic and N. Konjevic, *Characterization of an Atmospheric Pressure Pulsed Microjet*, 28th Summer School and International Symposium on the Physics of Ionized Gases, Beograd, Srbija, 29. avgust - 2.septembar 2016, str. 276-279
- Vinic M, Ivkovic M, *The emission enhancement in single pulse laser induced breakdown spectroscopy*, Proceedings of the 11th International Conference on Fundamental and Applied Aspects of Physical Chemistry, Belgrade (Serbia), September 24-26 2012, p. 134-136

Radovi na međunarodnim konferencijama štampani u izvodu M34

- M. Vinic, B. Stankov, *Spatial and temporal resolved study of some atmospheric pressure discharges*, Internacionalna konferencija studenata fizike (ICPS), Msida, Malta, 11.-17. avgust 2016, str. 64-65
- M. Vinic, M. Cvejic and M. Ivkovic, *Spatial and temporal characterisation of combined laser induced plasma and spark technique*, Book of Abstracts 7th Euro-Mediterranean Symposium on Laser Induced Breakdown Spectroscopy, EMSLIBS 2013 Bari (Italy), September 16-20 2013, p. 151

Radovi na domaćim konferencijama štampani u celini M63

- Vinić M, Ivković M, *Klasifikacija zemljišta primenom spektroskopije laserom indukovanoj proboja*, Zbornik radova XII Kongresa fizičara Srbije, Vrnjačka Banja, 28. april – 2. maj 2013, str. 404-407

Научном већу Института за физику

Предмет: Анализа научне активности Милице Винић

Научна активност кандидаткиње Милице Винић у Институту за физику усмерена је на испитивање процеса ласерске аблације до које долази приликом интеракције ласерског зрачења са материјалом при чему се формира плазма. Кандидаткиња се превасходно бавила анализом оптичког емисионог спектра плазме. Ова истраживања била су усмерена ка развоју спектроскопије ласером индукованог пробоја - ЛИБС (*Laser Induced Breakdown Spectroscopy*), која се примењује за одређивање састава различитих узорака. Основни недостатак ове методе су високе границе детекције услед малих интензитета уочених спектралних линија. Повећавање интензитета снимљених линија остваривано је применом додатног електричног пражњења иницираног ласерском аблацијом мете. У ту сврху, израђена је цев у коју је била постављена ротирајућа мета од легуре алуминијума. На крајевима цеви смештене су електроде од волфрама. У интеракцији ласерског импулса са метом долази до формирања иницијалне плазме, при чему се индукује пражњење између електрода. На овај начин постигнуто је додатно повећање температуре плазме, а самим тим и интензитета линија. Испитивања су вршена при различитим притисцима аргона, хелијума или ваздуха, са и без додатног електричног пражњења. Утицај наведених параметара огледа се у промени времена трајања плазме, као и у промени њене запремине и интензитета. Сви спектри су снимани у различитим временима трајања плазме, што је отворило могућност за утврђивање оптималних услова за снимање спектра у описаној конфигурацији.

Даљи рад кандидаткиње био је везан за примену ЛИБС са додатним електричним пражњењем за анализу различитих типова земљишта при атмосферским условима. Овакве врсте анализа су веома значајне у пољопривредној производњи јер се на основу карактеристика тла одлучује о врсти агротехничких мера којима треба третирати земљиште, а све у циљу квалитетније производње. Поменутом методом испитивана су четири различита типа земљишта, при чему је одређиван квалитативни састав земљишта. Квантитативни састав земљишта није било могуће одредити због недостатка одговарајућих стандарда. Применом компаративне методе одређен је квантитативни састав земљишта и на тај начин су потврђени резултати добијени применом ЛИБС са додатним електричним пражњењем. Пре спектроскопских мерења, простирање произведене плазме праћено је применом брзе фотографије са временском резолуцијом од 50 нс. Ова истраживања била су неопходна за одређивање оптималних услова за снимање спектра различитих врста мета. Утврђено је да постоје разлике у снимљеним спектрима, у зависности од изабране зоне снимања. У централном делу пражњења присутне су линије материјала мете, док се у периферним деловима, ближе електродама, поред наведених линија, налазе и линије материјала од којих су направљене електроде. Присуство ових линија знатно отежава анализу већ комплексног спектра, тако да је на почетку свих мерења било кључно одредити који део зрачења плазме треба снимати.

Поред ЛИБС технике, анализиран је и оптички емисиони спектар који се добија аблацијом зинова цеви (ВеО керамике) путем електричног пражњења. Ова истраживања била су усмерена ка добијању извора који би могао да послужи за безбедно посматрање линија берилијума, који је врло токсичан. Испитивања су вршена како са различитим електричним

конфигурацијама, тако и са различитим поставкама и варијантама самог извора док се није постигао резултат. Спектралне линије добијене применом оваквог извора зрачења коришћене су за израчунавање Штаркових параметара. На овом експерименту је први пут потврђено постојање забрањених компонената неких линија. Такође, приликом рада је запажено да под утицајем пражњења долази до формирања прашине берилијума. Оваква истраживања су од великог значаја за астрофизику - берилијум је присутан у великом броју звезда чије се зрачење прати. Ови подаци су важни и због фузионих истраживања. Тренутно је у изградњи ИТЕР (*International Thermonuclear Experimental Reactor*). Први слој зидова овог реактора, који је у директном контакту са формираном плазмом, биће направљен од берилијума. Високе температуре плазме могу довести до топљења, испаравања и формирања прашине берилијума. Ово би довело до оштећења зидова суда, али и до промене састава плазме. Експеримент је спроведен у циљу анализе процеса који доводе до формирања прашине.

Конструисан је и испитиван још један спектроскопски извор зрачења - плазма млаз. Извор плазма млаза је малих димензија - електроде се налазе на растојању од 1цм, а отвор на електроди, кроз који пролази плазма млаз, има дијаметар 0,6мм. Пропагација плазма млаза је праћена коришћењем брзе фотографије чиме је потврђено његово формирање и анализирано простирање. Анализирани су и упоређивани оптички емисиони спектри плазма млаза и цеви у којој се одвијало пражњење. Снимање се обављало истовремено, уз помоћ три фибера - један за снимање пражњења у цеви, други за снимање плазма млаза и трећи за *end on* снимке. На основу ових снимака било је могуће утврдити разлике у концентрацији и температури унутар саме цеви и у плазма млазу, као и колики је појединачни допринос ове две плазме у укупном сигналу. Пражњење је успостављано у више гасова, пражњењем кондензатора различитих капацитета. Мењане су димензије, отвор и растојање између електрода, а све у циљу добијања стабилног извора који се може корисити за анализу спектралних линија гаса. Утврђено је да овако конструисан извор не може бити употребљаван за третирање биолошких узорака због високе температуре и ниске електронске концентрације.

Као наставак истраживања, приступило се даљој модификацији ЛИБС технике, у циљу побољшања аналитичког сигнала. Ласерка аблација коришћена је као метод уношења узорака у различите изворе. Полазећи од идеје да би уношењем аблираног материјала у другу врсту пражњења добили линије мете већег интензитета и полуширине, ЛИБС техника је комбинована са тињавим пражњењем, са микроталасним изворима, високострујним пражњењима. Свака конфигурација је испитивана методом оптичке емисионе спектроскопије, при чему су снимци временски и просторно разложени. Даљи рад кандидаткиње усмерен је ка наставку започетих истраживања.



28th Summer School and International Symposium on the Physics of Ionized Gases

Aug. 29 - Sep. 2, 2016, Belgrade, Serbia

CONTRIBUTED PAPERS

&

ABSTRACTS OF INVITED LECTURES,
TOPICAL INVITED LECTURES, PROGRESS REPORTS
AND WORKSHOP LECTURES

Editors:

Dragana Marić, Aleksandar Milosavljević,
Bratislav Obradović and Goran Poparić



University of Belgrade,
Faculty of Physics



Serbian Academy
of Sciences and Arts

CHARACTERIZATION OF AN ATMOSPHERIC PRESSURE PULSED MICROJET

M. Vinic¹, B. Stankov¹, M. Ivkovic¹ and N. Konjevic²

¹*Institute of Physics, University of Belgrade, Belgrade, Serbia*

²*Faculty of Physics, University of Belgrade, Belgrade, Serbia*

Abstract. The results of an experimental study of atmospheric pressure pulsed microjets in helium and gas mixture are presented. The images of plasma jet propagation were recorded and emission spectra from glass discharge tube and plasma jet were analyzed and compared. From helium spectral lines electron density was calculated for several different configurations of discharge source. Temporal dependence of electron density was determined. The influence of various capacitors and discharge voltages on plasma jet emission and propagation were studied also.

1. INTRODUCTION

Atmospheric pressure He microdischarges have many different configuration and many applications. Most of them are constructed in order to obtain cold plasmas for medical and plasma chemical applications. It can be used for cleaning, decontamination, etching, or coating surfaces at atmospheric pressure and low temperature. [1] One reason for why plasma jets are advantageous is because even though the electrons are hot, the overall gas is at room temperature. Another important advantage of using atmospheric plasmas is the possibility to process materials which are not resistant to vacuum. [2,3] The main disadvantage of such microdischarges is high consumption of He.

Here, we present attempt to construct and characterize low flow atmospheric pressure He single pulse plasma microjet.

2. EXPERIMENT

Schematic sketch of pulsed atmospheric pressure plasma jet is shown in Figure 1a. The experimental setup consists of microjet, focusing optic, radiation intensity detection system (imaging spectrometer equipped with ICCD camera), computer and electronics system for synchronization, detector gating and spectrum storage, Figure 1b:

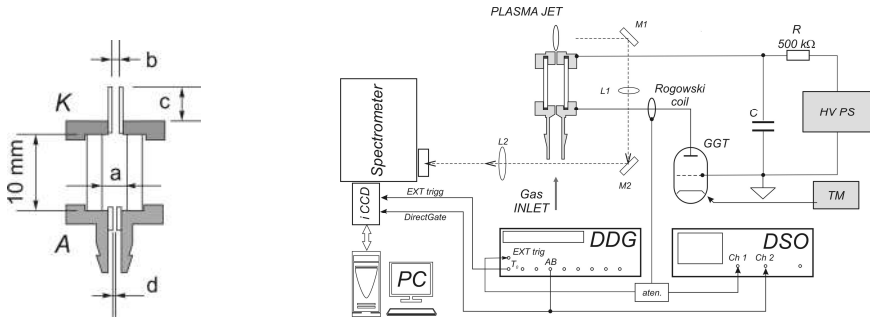


Figure 1. a) Microjet; b) Experimental setup.

Light emitted from microjet was focused by the use of lens L_1 having focal length of 32 cm. For the recordings of plasma jet images an additional lens L_2 was used having focal length of 17 cm.

Plasma image was projected on the 20 μm wide entrance slit of the 0.3 m imaging spectrometer Andor Shamrock 303, equipped with ICCD camera. The camera gating was performed with digital delay generator (DDG) by processing signal from Rogowsky coil which was used for current pulse measurements. The spectra were recorded at different delay times in respect to beginning of current pulse monitored by digital storage oscilloscope (DSO). The fast pulse discharge is driven by a different capacitors - C, charged with high voltage power supply - HV PS.

In microjet gas is fed through a hole in center of lower electrode (d), with passage trough glass tube and output through hole in an upper electrode (b) see Fig. 1a. Glass tubes with various inner diameters were used (a). In some cases, stainless steel tubes (SST) of different lengths were placed in upper hole (c), Table 1.

Table 1. List of different configurations of microjet.

label	MJ1	MJ2	MJ3	MJ4	MJ5	MJ6	MJ7	MJ8	MJ9	MJ10	MJ11	MJ12
a [mm]	4	4	4	4	4	4	2	2	1	1	1	2
b [mm]	0.50	0.70	0.70	0.70	0.70	0.45	0.70	0.45	0.70	0.70	0.45	0.5
c [mm]	0	6	15	0	6	6	6	6	0	6	6	0
d [mm]	0.50	0.10	0.10	0.35	0.35	0.35	0.35	0.35	0.35	0.35	0.35	0.35

First step of our experiment was to record plasma images. After analyzing images, next step was to record spectrum of main discharge and plasma jet area. Helium and gas mixture (He with 1.5% CO_2 and 1.5% N_2) were used as carrier gasses. For the electron density determination we used the separation between allowed and forbidden component of He I 447.1 nm line [4].

3. RESULTS AND DISCUSSION

Due to an insufficient space in this publication we show only several results out of large number of images and spectra recordings.

Images of jet propagation were recorded, see example in Figure 2. First image depicts emission from discharge tube and plasma jet. In order to record images of jet, emission from discharge tube was blocked. It was discovered that jet appears 1 μ s after beginning of discharge current, reaches maximum intensity at 2.5 μ s and lasts until 14 μ s. Based on these observations time and spatial position of subsequent measurements were selected. Another result from images appeared - in this type of discharge there is no plasma propagation, i.e. plasma stays in contact with upper electrode.

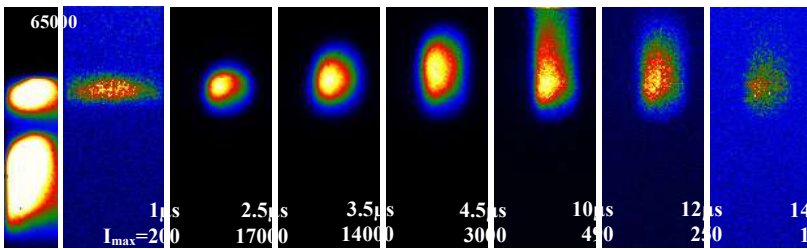


Figure 2. Images of jet evolution. Each image is normalized to max light intensity.

In order to obtain aperiodic waveform of discharge current the resistor (0.4 Ω) connected in series with discharge was used. Figure 3 illustrates different current waveforms depending on used capacitor and applied voltage:

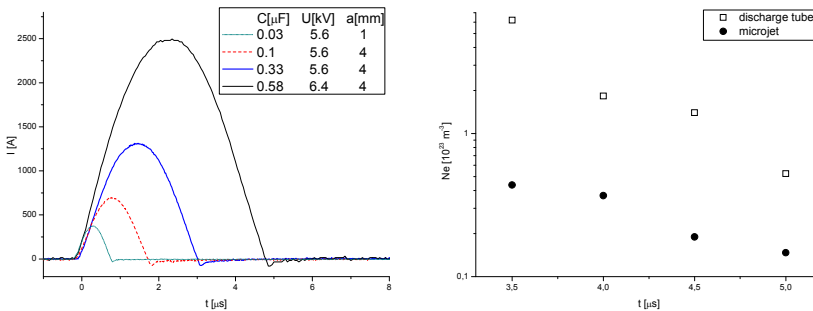


Figure 3. a) Current waveform depending of C and U; b) Temporal dependence of electron density for discharge tube and microjet (MJ12), C=0.33 μ F, U=3.6 kV.

Temporal dependence of Ne for microjet without SST is shown in Figure 3b. Strong continuum obstructed estimation of Ne at the beginning of discharge so first evaluated Ne value is at 3.5 μ s. At that moment, electron density in discharge tube is $6.2 \cdot 10^{23} \text{ m}^{-3}$, while Ne in jet is $4.4 \cdot 10^{22} \text{ m}^{-3}$.

The distinction between spectra from discharge tube and jet is shown in Figure 4a.

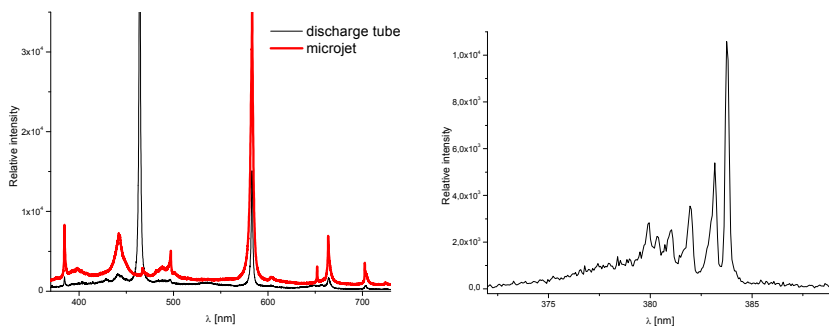


Figure 4. a) Comparison of spectra from discharge tube and microjet (MJ1), $C=0.33 \mu\text{F}$, $U=5.6 \text{ kV}$; b) N_2^+ FNS (MJ8), $C=0.33 \mu\text{F}$, $U= 5.6 \text{ kV}$.

Molecular bands of N_2 were detected in spectra when gas mixture was used as carrier gas, see Figure 4b. This is an indication that plasma jet temperature is low.

Acknowledgements

This work was financed by the Ministry of Education, Science and Technological Development of the Republic of Serbia under Project OI 171014 and TR 37019.

REFERENCES

- [1] M. Wolter, S. Bornholdt, M. Häckel, H. Kersten, *Journal of Achievements in Materials and Manufacturing Engineering* 37, 730 (2009)
- [2] Peter Bruggeman, Ronny Brandenburg, *J. Phys. D: Appl. Phys.* 46, 28 (2013)
- [3] M. Laroussi, T. Akan, *Plasma Process. Polym.* 4, 777 (2007)
- [4] M. Ivkovic, M.A. Gonzalez, S. Jovicevic, M.A. Gigosos, N. Konjevic, *Spectrochimica Acta Part B* 65, 234 (2010)



29th Summer School and International Symposium on the Physics of Ionized Gases

Aug. 28 - Sep. 1, 2018, Belgrade, Serbia

CONTRIBUTED PAPERS &

ABSTRACTS OF INVITED LECTURES,
TOPICAL INVITED LECTURES, PROGRESS REPORTS
AND WORKSHOP LECTURES

Editors:

Goran Poparić, Bratislav Obradović,
Duško Borka and Milan Rajković



Vinča Institute of
Nuclear Sciences



Serbian Academy
of Sciences and Arts

NANOPARTICLES ON A SAMPLE SURFACE AS LASER INDUCED BREAKDOWN SPECTROSCOPY ENHANCERS

M. Vinić^{1,2}, M. R. Gavrilović Božović¹, B. Stankov¹, M. Vlanić¹ and M. Ivković¹

¹*Institute of Physics, University of Belgrade, Belgrade, Serbia*

²*Faculty of Physical Chemistry, University of Belgrade, Belgrade, Serbia*

Abstract. Signal enhancement of Laser Induced Breakdown Spectroscopy in the presence of gold nanoparticles was studied. Nanoparticles were synthesised using pulsed laser ablation of the rotating Au target immersed in liquid mediums. Stability of nanocolloids was estimated. Nanosuspensions were applied to sample surface what enabled studies of Nanoparticle Enhanced Laser Induced Breakdown Spectroscopy. The effect of spectral line enhancement was observed under the optimised conditions both for neutral and ionic lines of the studied sample material.

1. INTRODUCTION

Laser Induced Breakdown Spectroscopy (LIBS) is emission spectroscopy technique that uses a short laser pulse to create plasma on the sample surface, and analyses formed plasma to gather information about the sample studied. Despite of all its advantages (fast response, no or minimal sample treatment, simple setup, requires only optical access to the sample), lower detection limit is the largest drawback of this technique. One way of signal enhancement is deposition of metallic nanoparticles on sample surface before laser irradiation. In this way, the order of magnitude enhancement of optical signal can be obtained [1,2].

In this work, nanoparticles (NPs) were synthesised using laser ablation of the bulk gold in liquid medium, and then applied on the surface of the sample. Surface prepared in such a way was then irradiated with the laser beam, Nanoparticle Enhanced LIBS (NELIBS) plasma was formed and spectra were recorded. It was shown that application of Au NPs on the target surface prior to laser induced breakdown leads to signal enhancement of sample's element optical emission.

2. EXPERIMENT

Experiment was conducted in several steps. Firstly, it was necessary to synthesize Au NPs, uniform by size and shape. Next, the size of the NPs needed

to be evaluated, based on the position of a Surface Plasmon Resonance (SPR) band maximum. In order to do that, absorption spectra of all produced colloids were recorded with spectrophotometer [3-5]. After that, synthesised colloids of NPs ought to be applied to analysed metal target (AlMgCu₅), where proper volume of the colloid drop and surface coverage had to be determined experimentally. As a final step, conditions for NELIBS spectra recordings had to be optimised.

Method of choice for NPs synthesis was laser ablation in different solutions. Experimental setup consisted of laser (Nd:YAG, 2nd harmonic 532 nm), mirror for guiding the laser beam (45° angle), focusing lens of 2.5 cm focal length and rotating table on top of which cuvette with a solution and immersed Au target were positioned., see Figure 1a. In order to find the optimal conditions for NPs generation, laser energy and wavelength were changed. Also, different distances between the target and lens were set, so different energy densities on the target surface were obtained, leading to the NPs of various sizes. Duration of ablation was varied in order to obtain different colloid concentrations. NPs were synthesized in water (distilled and deionized) and in different organic solvents (DMSO, Acetonitrile and Chloroform) [6]. Characterisation of formed nanocolloids was performed with measurements of SPR band using spectrophotometer Beckman Coulter DU720. Stability of formed solutions was also estimated.

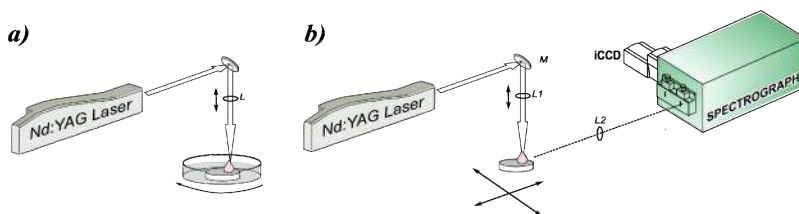


Figure 1. Experimental setup: a) for synthesis of Au nanocolloid; b) for NELIBS.

Experimental setup used for measurements of NELIBS spectra of prepared samples consisted of: laser (Nd:YAG, 2nd harmonic 532 nm), mirror (45° angle), focusing lens of 2.5 cm focal length (L_1) and lens for focusing NELIBS plasma (L_2 , $f=20\text{cm}$) onto the entrance slit of detection system (imaging spectrometer equipped with ICCD camera), see Figure 1b. Position of the projection lens L_2 with respect to the spectrometer was varied, i.e. different portions of the plasma volume were collected by optical system, which had prove to have direct consequence on the spectral line emission enhancement.

3. RESULTS AND DISCUSSION

When a metal particle is exposed to light, the oscillating electromagnetic field induces a collective coherent oscillation of conduction band electrons. The amplitude of the oscillation reaches maximum at a specific frequency, called surface plasmon resonance. The SPR induces a strong absorption of the incident light and thus can be measured using a UV-Vis

absorption spectrometer [5]. Based on the measured position of SPR band maximum, sizes of Au NPs were estimated, see Figure 2a. After few days, recordings were repeated in order to verify stability of solutions, Figure 2b. The variations in position of the SPR maximum were almost negligible after two days, leading to the conclusion that produced colloids are rather stable. Significant change in the SPR maximum position was only detected four days after the colloid synthesis.

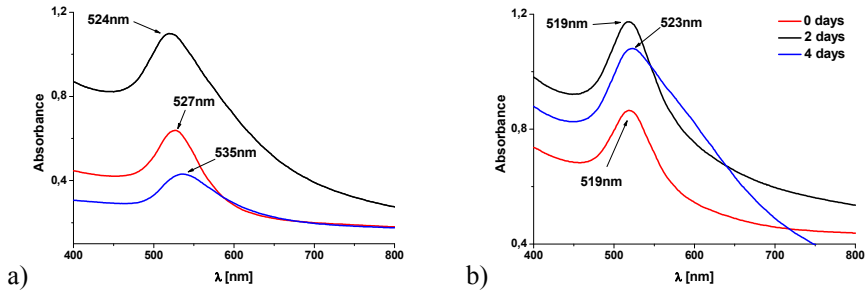


Figure 2. SPR band of formed solutions: a) size estimation; b) stability check.

Estimated sizes of Au NPs (30 ± 5 nm) [3] were in the range of sizes that have already been reported to produce NELIBS effect [1], even two days after synthesis. Besides NPs size, important parameter for line intensity enhancement is the NP surface concentration. It was found that after certain limit, further increase of concentration does not contribute to signal enhancement [2]. In order to test that, nanocolloid was first applied on the sample surface in a form of large droplets ($\sim 10 \mu\text{l}$). In this case, the deposition of colloid was inhomogeneous such that the concentrations at the edges were higher than at the center, i.e. “coffee-ring” effect [7], resulting in noticeable enhancement only when particular place on a drop was irradiated. This indicates that, with the large droplets, surface concentration of NPs was above critical, leading to decreased NELIBS performance [7]. Since enhancement is strongly dependent on the total amount of colloid, smaller droplets should be used. Having this in mind, further on microdroplets ($0.5 \mu\text{l}$) were applied with micropipette on the previously irradiated surface of the target.

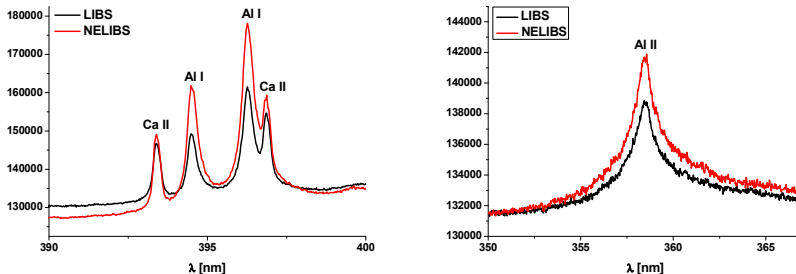


Figure 3. Comparison of LIBS and NELIBS spectra for neutral and ionic lines of main target constituent.

Spectra obtained with microdroplets are shown in Fig. 3. All presented spectra were recorded with single shot. Further enhancement of optical signal could be obtained if signal accumulation was performed. Increase of signal intensity was present in both neutral and ionic lines. Enhancement of spectral line intensity was more pronounced in case of neutral lines, possible due to larger emission volume of NELIBS plasma. Since LIBS and NELIBS plasma have similar plasma parameters [1], larger emission volume of NELIBS plasma means more contributions from "colder" layers which are emitters of mostly neutral lines. It is important to emphasize this was the reason why lens L_2 was positioned in such a way that complete plasma volume was focused to the spectrometer. This configuration corresponds to the maximum signal enhancement.

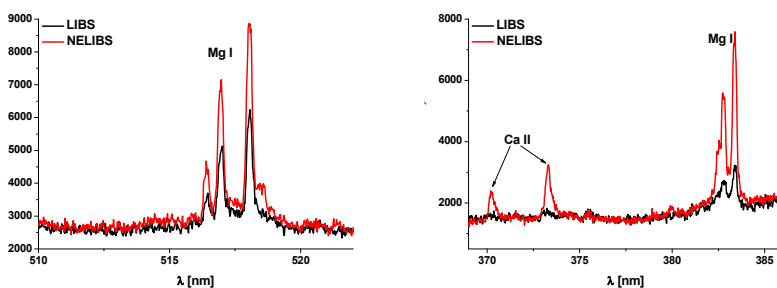


Figure 4. Comparison of LIBS and NELIBS spectra of minor elements in sample.

Fig. 4 illustrates intensity increase of spectral lines of magnesium which is minor sample constituent. Also, lines of Ca appeared in NELIBS spectra. Calcium can be present in AlMgCu_5 in small amounts, but also can come from water used as a medium during the NPs synthesis. Because of this uncertainty, it can be concluded that this method is not reliable for investigations of calcium containing samples.

Acknowledgements

This work was financed by the Ministry of Education, Science and Technological Development of the Republic of Serbia under Projects OI 171014 and TR 37019. Special thanks to Zoran Velikić who helped in performing spectrophotometric measurements.

REFERENCES

- [1] A. De Giacomo et al, *Spec. Acta Part B* 98, 19 (2014)
- [2] A. De Giacomo et al, *Anal. Chem.* 88, 9871 (2016)
- [3] S. Link and M. A. El-Sayed, *J. Phys. Chem. B* 103, 4212 (1999)
- [4] V. Amendola et al, *J. Phys.: Condens. Matter* 29, 203002 (2017)
- [5] X. Huang and M. A. El-Sayed, *J. of Adv. Research* 1, 13 (2010)
- [6] V. Amendola et al, *J. Phys. Chem. B* 110, 7232 (2006)
- [7] C. Zhao and D. Dong, *Anal. Chem.* 88, 9869 (2016)

Novel plasma source for safe beryllium spectral line studies in the presence of beryllium dust

B.D.Stankov^{a,b}, M.Vinić^a, M.R.Gavrilović Božović^a and M.Ivković^a

^aInstitute of Physics, University of Belgrade, P.O.Box 68, 11080 Belgrade, Serbia

^bUniversity of Novi Sad, Faculty of Sciences, Department of Physics, Trg Dositeja Obradovića 4, 21000 Novi Sad, Serbia

Abstract

Plasma source for beryllium spectral line studies in the presence of beryllium dust particles was realised. Guideline during construction was to prevent exposure to formed dust, considering the toxicity of beryllium. Plasma source characterization through determination of optimal working conditions is described. The necessary conditions for Be spectral lines appearance and optimal conditions for line shapes measurements are found. It is proven experimentally that under these conditions dust appears coincidentally with second current maximum. The electron density measured after discharge current maximum is determined from the peak separation of the hydrogen Balmer beta spectral line, and the electron temperature is determined from the ratios of the relative intensities of Be spectral lines emitted from successive ionized stages of atoms. Maximum values of electron density and temperature are measured to be $9.3 \cdot 10^{22} \text{ m}^{-3}$ and 16800 K, respectively. Construction details and testing of BeO discharge tube in comparison with SiO₂ and Al₂O₃ discharge tubes are presented in this paper also.

Corresponding author mail: milivoje.ivkovic@ipb.ac.rs

Keywords: optical emission spectroscopy, spectral line shapes, plasma sources, dusty plasma, beryllium spectral lines

1. INTRODUCTION

The interest for Be spectral lines studies stems from the prevalence of Be, which occurs in nature and is used in many devices. Beryllium is element which has six times the specific stiffness of steel and at the same time it's one-third lighter than aluminum. This unusual combination of properties makes it suitable for a wide range of applications: aerospace, military, information technologies, energy exploration, medical and other advanced applications. The three most used forms of beryllium are beryllium-containing alloys, pure beryllium metal and beryllium ceramics, also known as beryllium oxide ceramic.

Since Be is also naturally occurring element in metal-poor stars [1] study of the spectral lines emission of beryllium is important for astrophysics. For example, spectral lines coming from Be II deexcitation at 313.0 nm and 313.1 nm, are used for the analysis of some stars origin [2]. Hence, basic knowledge about beryllium spectral emission is available but still, according to critical reviews [3-9], spectroscopic investigations and Stark parameters studies are almost exclusively limited to Be II resonance lines at 313 nm [10-13]. In several of these studies [10-12] plasma source was electromagnetically driven "T" tube. Beryllium was deposited in the form of thin layers of BeCl₂ on the electrode [10, 11] and by dusting the quartz tube with BeCl₂ [12]. As for [13] beryllium was deposited in the form of chlorides on the electrode of Z pinch.

Because of its low atomic number and very low absorption for X-rays, the oldest and still one of the most important applications of beryllium is in radiation windows for X-ray tubes [14, 15].

Also, the beryllium has been chosen as the element to cover the first wall of ITER (International Thermonuclear Experimental Reactor). The first wall of ITER is a part of the blanket that is constructed with 440 panels that completely cover inner wall of the vacuum vessel. Those panels will be covered with 8-10 mm of beryllium armor, leading to approximately 12 tons of beryllium in total, distributed over a surface area of about 700 m² [16, Sec. 13.3.1.2]. In addition, Beryllium oxide is also used as insulation in some ITER components [16, Table 13.3-1]. Beryllium is material of choice in ITER due to its light weight, low tritium absorption and efficient trapping of oxygen impurities at its surface forming BeO. The drawback of Be is its low melting temperature what makes it vulnerable to edge-localized modes (ELMs) and disruptions [17]. ELMs and disruptions may provoke large thermal transient loads on beryllium components of the first wall leading to rapid heating of beryllium surface. Rapid heating can result in plasma-surface interaction processes and can lead to material loss, melting, evaporation and formation of beryllium dust. Erosion of beryllium under transient plasma loads will determine a lifetime of ITER first wall [18]. The presence of dust particles in fusion reactors has several consequences. There is a safety issue because Be is toxic in case of inhalation, so constant air monitoring must be provided [19]. Other problems regard the pollution of the plasma by particles, causing the reduced performance, or its deposition on diagnostic equipment. Still, the knowledge of dust creation processes and behavior in a plasma environment is very limited [20], partially due to the previously mentioned safety issues when handling plasma sources with toxic materials, as beryllium.

Research on dusty plasma is gaining in popularity due to its unique properties and importance for novel technologies [21]. Furthermore, the dust in plasma shows interesting fundamental phenomena like plasma crystals and dust acoustic waves [22-24]. In many applications, besides already mentioned ITER, the dust in plasma is unwanted effect, e.g. for plasma etching and thin film

deposition in semiconductor industry. This increases the relevance of dust particle formation studies and sets the need to relate it to some other physical phenomenon, like spectral emission from the tokamak plasma [25, 26].

In addition, in situ examination of plasma facing materials in tokamak (beryllium and others) by laser induced breakdown spectroscopy – LIBS [27, 28] requires the knowledge of their atomic data (transition probabilities, Stark broadening parameters etc.). Lack of Stark parameters for Be spectral lines was one of the main inspirations for this plasma source construction.

The main goal of this work was not only to obtain stable plasma source for beryllium spectral lines study, but also to enable examination of dust particles influence on emission spectra when optimal conditions for Be spectral emission are achieved. The idea was to obtain beryllium spectral lines from erosion of the beryllium oxide, BeO discharge tube, and preferentially, the lines belonging to transitions other than resonant, which are the only ones studied in detail up to now. To draw an analogy with previous studies [10-13], in set up we used, beryllium was introduced through the ablation of a ceramic tube settled inside the discharge tube, which allowed more consistent ablation, longer and more reliable work, and appearance of various Be spectral lines. In order to closer investigate the influence of specific discharge tube material on dust particle production and emission spectra, two additional discharge tubes were made. Construction details and testing of BeO discharge tube in comparison with SiO₂ and Al₂O₃ discharge tubes are also presented in this paper.

2. EXPERIMENT

Experimental setup is presented in Fig. 1. Capacitor C is charged between 4 and 8 kV, using high voltage power supply, HV PS, operated through the laboratory made high voltage control. When voltage reaches selected value, the pulse is generated by high voltage control and shaped by the trigger unit in order to initiate ignitron switch, which starts the current flow through linear pulsed discharge tube. The current shape is monitored by Rogowski coil and recorded with digital storage oscilloscope, DSO (Tektronix TDS 360), see typical current shapes for different discharge tubes in Fig. 2a. The same but attenuated signal from the Rogowski coil is used for the triggering of ICCD camera (Andor DH720), see Fig.1. The acquisition gate width, t_G and delay, t_D are determined with digital delay generator, DDG (Stanford Research Systems SRS, Model DG535). The spectra are recorded using gate width of 50 ns at different delays in order to determine temporal evolution of plasma parameters.

The 1:1 image of the radiation emitted end-on along the axis of the discharge tube is projected on the entrance slit (20 microns wide) of the Shamrock 303 (Andor) imaging spectrometer using folding mirrors M₁ and M₂ and quartz achromatic lens (focal length $f = 33$ cm). The change of the diffraction grating (300, 1200 or 2400 groves/mm), slit width and wavelength position are performed using commercial Andor Solis software. The instrumental width with 2400 g/mm grating and 20 μ m slit width, determined using Oriel penlight calibration lamps is 0.09 nm.

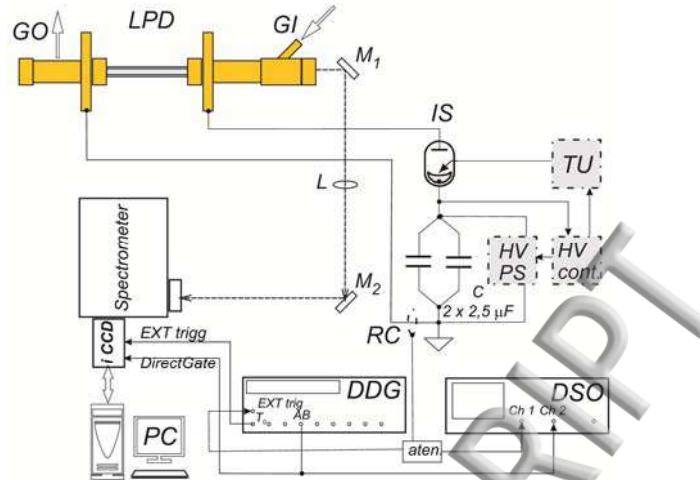


Figure 1. Experimental setup, LPD- linear pulsed discharge, GO- gass outlet, GI- gass inlet, M_1 – mirror, L- lens, M_2 - mirror, IS- ignitron switch, TU- trigger unit, HV PS - high voltage power supply, RC- Rogowski coil, DSO - digital storage oscilloscope, DDG - digital delay generator, ICCD – Intensified Charge Coupled Device camera, PC – personal computer

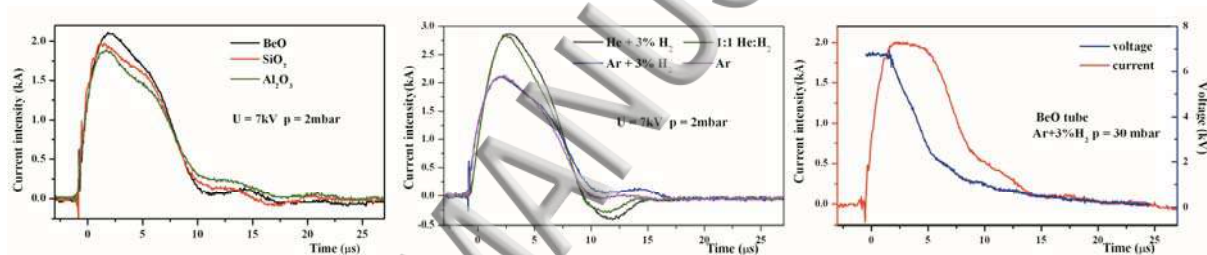


Figure 2. Current shapes for: a) different discharge tubes for the same gas type $Ar+3\%H_2$, pressure $p=2$ mbar, and discharge voltage $U=7$ kV, b) BeO tube with different gasses at same pressure 2 mbar and same voltage 7 kV c) temporal evolution of voltage and current for BeO tube and $Ar+3\%H_2$

3. EXPERIMENTAL DETAILS AND PROCEDURE

The discharge tube was made and studied under different experimental conditions. Electrode material and dimension, electrodes separation, discharge voltage, initial discharge pressure and direction of various gas flows through the tube, see Fig. 3, were alternated. General layout and construction details of discharge tubes with special attention on safety measures are given first in 3.1, followed by the electrical characterization and optimization of the discharge in 3.2. Influence of discharge parameters on emission spectra is fully described and discussed in the Sect 3.3, while appearance and some properties of the dust particles formed during the discharge operation are described in the Sect. 3.4.

3.1. Construction details of the discharge tubes

According to Material Safety Data Sheets, MSDS [29], beryllium, BeO and especially their dust are highly toxic, and must be handled with great precautions. Therefore, the BeO discharge tube with inner diameter 2.6 mm, outer diameter 10 mm and overall length of 130 mm was settled inside the Pyrex glass tube with inner diameter 11.5 mm, outer diameter 14 mm and overall length of 140 mm, see Fig. 3a. In such a way, exposure of the beryllium tube to atmosphere was prevented. Position of the inner (ceramic) tube inside the outer (glass) tube was adjusted using Teflon rings or Teflon tape, see Fig. 3a. This extra space prevented cracking or destruction of the tube due to significant mismatch in thermal expansion coefficient between Pyrex glass and BeO tube and/or destruction caused by shock waves generated by pulsed discharge.

Several additional safety measures were undertaken to prevent exposure to beryllium oxide components and especially to BeO dust. When handling BeO tube, the surgical gloves, surgical mask, laboratory coat and goggles were used. Assembling and manipulation of the discharge tube were performed in the fume hood of the chemical part of the laboratory.

The discharge tube connectors had gas inlet or outlet port and electrode holder in the middle, ending with Wilson connectors for vacuum tight connection on one side, and quartz windows for spectroscopic observations on the other side, see Fig. 3b. The position of the high voltage connections and electrically isolated support is also presented in Fig. 3b. Discharge tubes worked under low pressure continuous gas flow. The gas was supplied from gas cylinder using regulation and needle valve, with continuous monitoring of gas pressure on the inlet side of the tube. Two positions of the tube inlet were tested, 90° angle and 45° angle relative to the discharge tube axis. The liquid nitrogen cooled trap and HEPA (high efficiency particulate air) filter were inserted in the front of and at the exit of the rotary vane vacuum pump. Gas exhaust from the vacuum pump was lead to the pump settled outside the laboratory and equipped with additional filter.

Two additional tubes were used for the comparative study of the discharge tube material influence on the dust generation. The first one, made of alumina ceramics, Al_2O_3 , with inner diameter 2.6 mm, outer diameter 10 mm and overall length of 125 mm was settled inside the glass tube with the same dimensions as the one used for the BeO tube. The second one, made of quartz, SiO_2 , with inner diameter 3 mm, outer diameter 6 mm and overall length of 140 mm was attached with an additional adapter to the same construction, see Fig. 3c. In the Fig. 3a the inner diameter of the hollow electrodes, d is presented. Throughout the experimental course of the study value of d was changing between 0.6 mm and 2 mm.

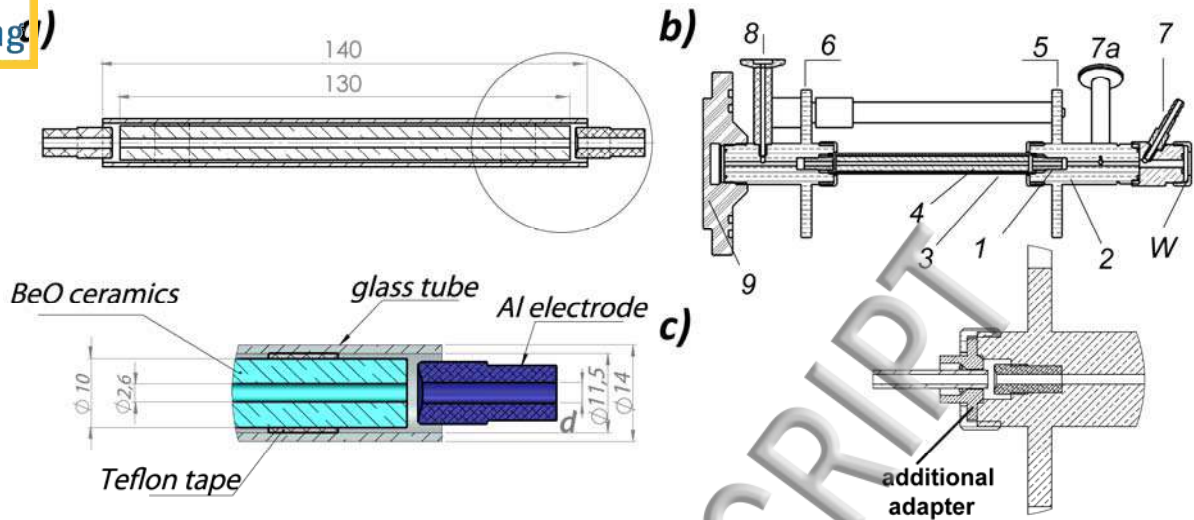


Figure 3. a) Construction of the BeO tube and its position inside the glass tube, b) discharge tube: (1) electrode, (2) holding body, (3) Pyrex glass tube, (4) tube made of BeO or Al_2O_3 , (5) anode connection, (6) cathode connection, (7) gas inlet at 45° angle, (7a) gas inlet at 90° angle, (8) gas outlet, (9) dielectric support, c) additional adapter used for SiO_2 tube.

3.2. Electrical characterization and optimization

In this study different gasses (Ar, Ar with 3% of H_2 , He + 3% of H_2 and 1:1 He/ H_2 mixture) at different pressures (1, 2, 3, 4, 5, 10, 20 and 90 mbar) were used. As the first step Paschen curves were determined, and then current shapes were recorded for each gas/pressure/voltage combination. Typical examples of voltage and current shapes are presented in Fig. 2. Current shapes for different tube materials at the same conditions are presented in Fig. 2a. Comparison of current shapes for BeO tube with different gasses is illustrated in Fig. 2b. Temporal evolution of voltage and current for BeO tube are also presented in Fig. 2c. As can be seen from the current curves in Fig. 2, the duration of the current pulse was around 10 μs , while current maximum was detected around 3 μs . Besides basic condition that, the discharge voltage must be larger than breakdown voltage, its value should be chosen in a way that parasitic discharge in the space between ceramic and glass tube, see Fig. 3a, is avoided. Such discharge may not only introduce spectral lines of impurities in the recorded spectrum, but also burn the Teflon tape and cause total destruction of discharge light source. In order to prevent this phenomenon, the discharge tube was first constructed in such a way that electrodes come in the ceramic tube see Fig. 3. Therefore, the part of the electrode that goes inside ceramic tube must have outer diameter smaller than 2.6 mm, limiting the maximum inner diameter of the electrode to 1.5 mm. Such electrodes also centre the ceramic tube inside the glass tube. However, the parasitic discharge still appears, Sec. 3.1. In addition, the optical signal from discharge tubes with such electrodes had very low intensity and poor reproducibility. Therefore, further measurements were performed with construction having a small separation between ceramic tube and electrodes, and with the Teflon rings being placed towards the middle of the discharge tube. In this configuration, parasitic discharge has never appeared.

Three types of electrodes were tested. Firstly, the electrode made of tungsten with opening of $d = 0.6$ mm, described earlier [30] was used. The idea was to obtain plasma with higher electron

densities and additional plasma emission from the plasma jet at outer side of the electrode, see [31], in order to use spectral line emitted from the plasma jet as a reference line for wavelength shift measurement. Unfortunately, spectral lines of the beryllium from jet were not detected, while the radiation intensity was very low and, in addition with a poor reproducibility. The spectra recorded using aluminum alloy electrodes with inner diameter 2 and 3 mm showed similar behavior irrespective of diameter, while signal to noise ratio was higher with larger electrode openings. Therefore, all further measurements were performed using aluminum alloy electrodes with 3 mm inner diameter. It should be stressed that under used experimental conditions spectral lines of the electrode material (tungsten and aluminum alloy AlMgCu₅) were not observed in the case of BeO and Al₂O₃ tube.

For the optimal conditions for BeO tube, see Sect. 3.3.2., the maximum current value goes up to 2.1 kA. The current minimum (observed in the case of He/H₂ mixtures) is caused by the change of plasma impedance resulting in periodic current pulse behavior. Namely, the resistor in the discharge circuit was chosen to obtain aperiodic current pulse with Ar, which is not optimal for discharge with He. The origin of the second maximum detected only when working with Ar and Ar with 3% H₂, see Fig. 2, is somewhat more complex and it will be addressed later in Sec. 3.4.

Here, one should notice that for different inner diameters of BeO, Al₂O₃ and SiO₂ tubes, current densities through the discharge tubes are different as well: 98 A/mm² for BeO, 87 A/mm² for Al₂O₃ and $j = 69$ A/mm² for SiO₂. Taking into account different tube lengths, the energy densities are: 0.058 J/mm², 0.06 J/mm², 0.046 J/mm² for BeO, Al₂O₃ and SiO₂ tubes, respectively.

3.3. Spectra recordings

Since the main objective of this work was the construction of safe and stable plasma source for beryllium spectral lines recording, the next step was to examine the change of the spectra under different discharge conditions. Construction details (d , gas flow direction), gas type and gas pressure, discharge voltages etc. were varied and their influence on recorded spectra was monitored. All spectroscopic studies were performed in three steps. The position of projected plasma image on the ICCD sensor was checked through the recordings with fully open slit of the imaging spectrometer and with the grating in the zero diffraction order. Afterwards, overall spectra were recorded with the shortest possible delay from the beginning of the current pulse (800 ns in this experiment, determined by reliable triggering of ICCD camera) using gate widths of 50 ns. Finally, temporal evolution of the spectra under various conditions was obtained and influence of the particular discharge condition studied. Influence of the different construction geometries on discharge operation has already been addressed in Sect 3.1 and 3.2 while here the impact of the gas type, pressure, flow and different applied voltages on the quality of spectral emission is inspected more closely.

3.3.1. Discharge gas

To study the influence of the gas type on spectra recording, i.e. on appearance of the tube material's spectral lines, three carrier gasses were used, He with 3% H₂, Ar and Ar with 3% H₂. 1:1 He/H₂ mixture was excluded from further measurements since beryllium lines were difficult to detect. Helium was chosen as one of the possible solution for carrier gas because it has small amount

of spectral lines, while hydrogen is added for diagnostic purposes, since it enabled diagnostics of electron density using separation of hydrogen Balmer beta line-peaks method [32]. At 1 mbar of gas pressure, capacitor $C = 5 \mu\text{F}$ charged to 7 kV, and delay of 12 μs , spectral lines of Be were narrower and had much lower intensity for He + 3% H₂ in comparison to Ar and Ar with 3% H₂, see Fig. 4. With He + 3% H₂ as a carrier gas, only prominent lines of Be appeared in current decay and lasted only few μs . In contrast, with Ar and Ar with 3% H₂, lines of Be lasted 8 μs longer. The highest intensity of Be lines was obtained using Ar/H₂ mixture. Therefore, all proceeding measurements were conducted using Ar with 3% H₂.

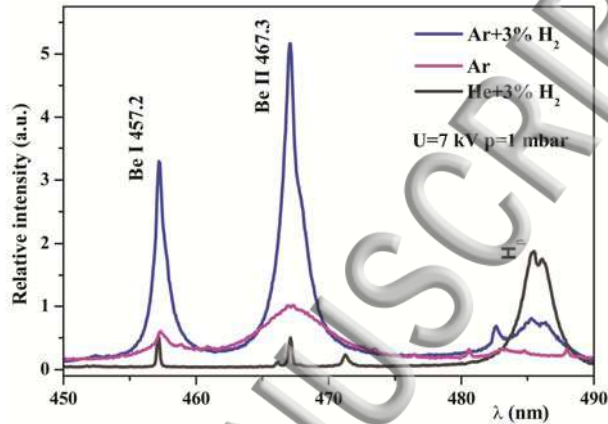


Figure 4. Influence of different gasses, Ar with 3% H₂, Ar and He with 3% H₂, on spectral line shapes of beryllium lines and the hydrogen Balmer beta, at discharge voltage 7 kV and pressure 1 mbar, delay 12 μs

Under certain conditions, discussed later in Sec. 3.4, the dust of discharge tube material was produced and often accumulated in small electrode openings (if smaller than 2 mm). These particles prevented evacuation of the discharge tube. In addition, with electrodes with 3 mm opening the dust particles were reaching the observation window, causing degradation of transmittance and lowering of the optical signal. Since the increase of the gas flow rate did not eliminate deposition of dust particles on the observation window, the gas flow direction was reversed, see Fig. 3b. Also, the additional adapter inlet enabling gas flow under the 45° angle was introduced; see Fig. 3b, which also helped in preventing dust particle deposition on the window. It was confirmed that the change of the gas flow direction did not affect the spectra recordings, so for the rest of the measurements gas was flowing from the output window towards the discharge tube support.

3.3.2. Discharge voltage and gas pressure

Spectra recorded for the same gas, pressure and gate width but different discharge voltages vary significantly. Namely, the differences between spectra were reflected in line intensity, line width and in appearance of non-beryllium lines. As can be seen in Fig. 5a, at 7 kV voltage, the beryllium lines are clearly distinguishable, while Ar lines are not observed at delays greater than 10 μs , i.e. after the current pulse. On the contrary, at discharge voltage of 5 kV, spectra are rich in spectral lines of discharge gas. Spectral lines of the gas appeared during and lasted after the current pulse, while spectral lines of the tube material were not observed, Fig. 5b. That's probably due to

low abrasion i.e. low quantity of beryllium in the plasma, or due to overlapping of Be spectral lines with stronger lines of Ar. The same is to be expected when using voltages less than 5 kV. Even though dust particles are produced at voltages of 7 kV, only at higher voltage of 8 kV they were deposited on the glass windows, lowering optical transparency in spite of all undertaken measures described in 3.3.1. Therefore, all forthcoming measurements were performed at discharge voltage of 7 kV.

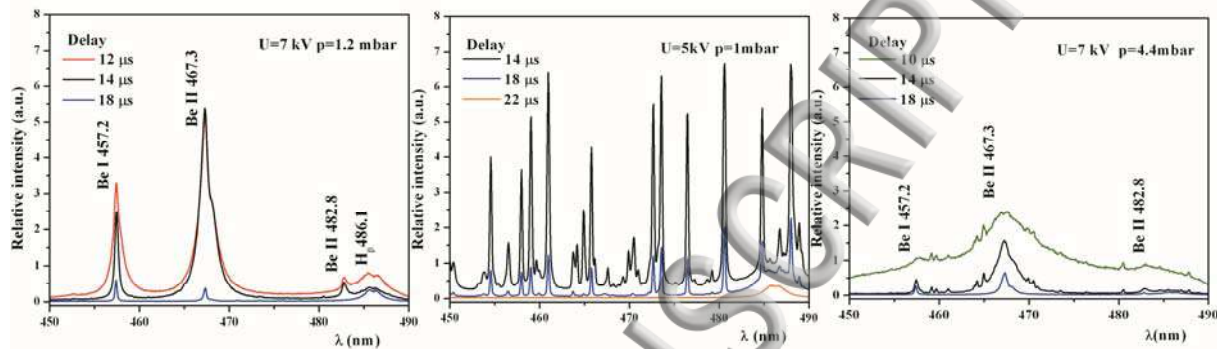


Figure 5. Influence of different discharge voltage and pressure on spectral line shapes of beryllium in argon with 3% of hydrogen

Gas pressure influences greatly the Be spectral lines intensity. A slight increase of pressure leads to more effective excitation of argon and appearance of argon lines in spectra. At pressure of 4.4 mbar shown in Fig. 5c, the spectral lines of Be are broader and continuum is more pronounced, compared to Fig. 5a. This is the most probably due to the increase of electron density. On the other hand, intensity of Be lines is lower, and argon lines are observed. Here, one should have in mind that spectral line at 467.3 nm presented in Fig. 5 is the most intense beryllium line recorded in this study i.e. that other spectral lines have very low intensity, if observed at all at pressure of 4.4 mbar and higher. Therefore, all proceeding measurements were conducted at pressure of 1.2 mbar in order to record spectral lines of beryllium.

Temporal evolution of spectra recorded between 330 nm and 660 nm with beryllium tube is presented in Fig. 6. The spectra were recorded for the conditions described earlier i.e. Ar with 3% H₂ and gas pressure 1.2 mbar (gas discharge voltage 7 kV), which were found to be optimal. At early delays (around 10 μ s), see Fig. 6, spectral lines of argon and pronounced continuum were evident. After current pulse, the intensity of spectral lines of discharge tube material was increasing reaching maximum value approximately at the time of the second maximum of the current pulse, see Fig. 2. Maximum intensity of the tube material's spectral lines was detected around 12 μ s. At that time lines of Be were prominent and Ar spectral lines were not detected. The beryllium lines were detected in spectra up to 25 μ s.

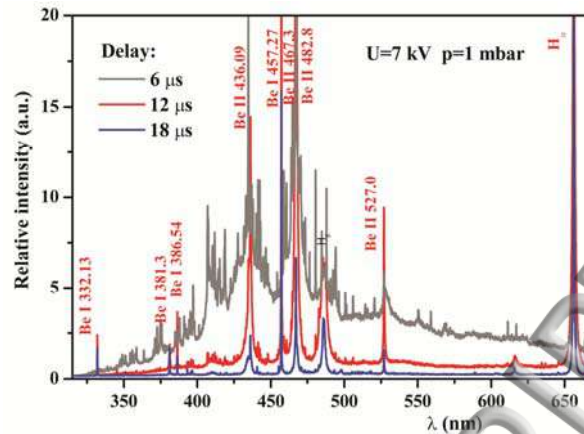


Figure 6. Temporal evolution of the spectra between 320 nm and 660 nm in low pressure pulsed discharge with beryllium tube

3.3.3. Comparison of plasma spectrum recorded from different tube materials

As mentioned previously, three different tube materials were used. Emphasis is placed on BeO tube, while spectra obtained using tubes made from SiO₂ and Al₂O₃ were used for comparison. In Fig. 7, spectra recordings with the tubes made of different materials are presented. The optimal conditions for measuring line shapes of Be were concluded to be at $C = 5 \mu\text{F}$, $U = 7 \text{ kV}$, gas Ar +3% H₂, $p = 1.2 \text{ mbar}$. At those same conditions spectral lines of Al emitted from Al₂O₃ tube were self-reversed, in consequence of self-absorption; while spectra when using SiO₂ tube could not be recorded because of occasional glass tube breaking and saturation of optical signal, even with the shortest gate. The best line/continuum ratio for recordings with glass SiO₂ tube was achieved at $C = 5 \mu\text{F}$, $U = 4 \text{ kV}$, gas Ar + 3% H₂, $p = 3 \text{ mbar}$, while for the Al₂O₃ tube those conditions were at $C = 5 \mu\text{F}$, $U = 6 \text{ kV}$, gas Ar +3% H₂, $p = 1.5 \text{ mbar}$.

Temporal evolutions of spectral lines emitted from tube material differ for all three cases. In early times (during the current pulse) there were no spectral lines of Be or they were not resolved due to overlapping with numerous much stronger Ar lines and intense continuum, see Sec. 3.3.2. Spectra of lines emitted from the SiO₂ and Al₂O₃ tubes were impossible to record at early delays due to the more intense continuum, which caused saturation of optical detector even at shortest gate time. As mentioned in 3.3.2., the lines of beryllium were detected in spectra up to 25 μs delay. The lines emitted when using SiO₂ and Al₂O₃ tubes were more persistent and they were observed in spectra up to 40 μs delay. In spectra obtained with SiO₂ tube, two very narrow aluminum lines coming most probably from aluminum alloy (AlMgCu₅) electrodes were detected. Spectral lines from the electrode's material did not appear in BeO tube's spectra. The dust particles were formed in all three cases.

From the results of the spectroscopic studies with tubes made of different materials and at various plasma conditions one can conclude that, if the space between discharge tube and electrodes exist cooler discharge region is formed which enables study of self-absorbed line shapes.

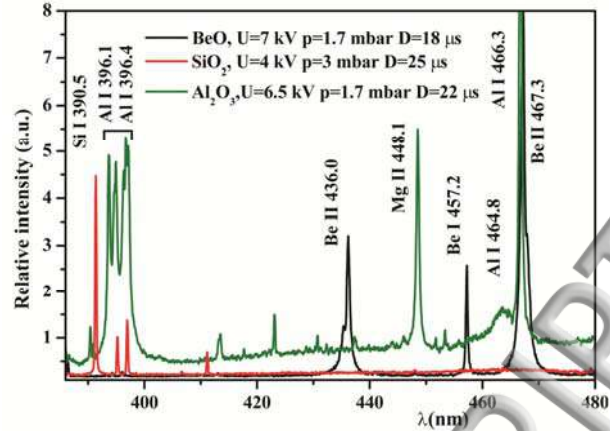


Figure 7. Comparison of spectra from low pressure pulsed discharge observed for three different tubes under optimized conditions

3.3.4. Plasma diagnostics

In order to characterize plasma source, the electron density, N_e , and temperature, T_e , were determined by iterative method.

The electron number density during plasma afterglow was estimated using peak separation $\Delta\lambda_{ps}$ of hydrogen Balmer beta line by using formula (6) from [32]:

$$\log N_e [m^{-3}] = A + B \log \Delta\lambda_{ps} [nm] = 22.65 + 1.53 \log \Delta\lambda_{ps} [nm] \quad (1)$$

In order to use that formula, the value of T_e was presupposed to be $13\,000 \pm 3\,000$ K, and based on the T_e , corresponding value of parameters A and B were taken from [32]. Using this range of T_e , the uncertainty of the N_e was 30%. For, in such a way determined electron number densities, the temperature was estimated from ratio of Be II 467.3 nm / Be I 457.3 using formula (2):

$$\frac{I_1}{I_2} = \frac{h^3}{2(2\pi mk)^{3/2}} \frac{(gA)_1 \lambda_1 N_e}{(gA)_2 \lambda_2 T_e^{3/2}} \exp\left(\frac{E_2 - E_1 + E_1^{ion} - \Delta E}{kT_e}\right), \quad (2)$$

where E_1^{ion} is ionization potential and ΔE is ionization potential lowering.

After few iteration N_e and T_e were determined. Transition probabilities were taken from NIST database [33].

Succeeding the determination of the excitation temperature and electron density, it is necessary to check if the conditions for LTE have been met. The expression (12) from [34] in the case of beryllium sets the boundary value of the electron concentration to be $2.85 \cdot 10^{22} m^{-3}$ for the temperature of 14200 K. This means that the conditions for the complete LTE in the plasma used in this experiment have been met. Given that only three neutral and three ionic spectral lines were recorded, and considering that those transitions have very similar upper level energies, use of Boltzmann plot could not provide more precise values of N_e and T_e .

The temporal evolution of T_e and N_e during plasma afterglow is presented in Fig. 8.

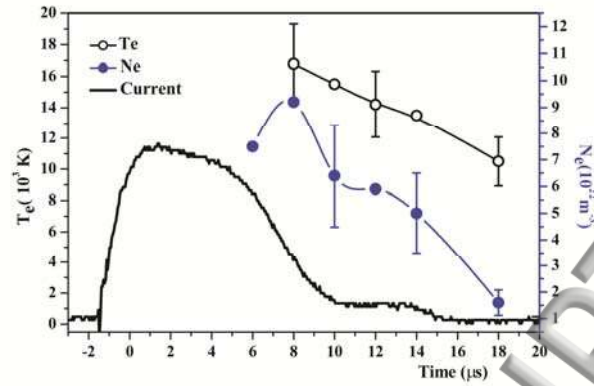


Figure 8. Evolution of T_e and N_e . N_e is determined from peak separation of hydrogen Balmer beta line [32] and T_e is estimated using ratio of intensities of beryllium lines, Be II 467.3 nm and Be I 457.3.

It can be seen from Fig. 8. that N_e has increased after the end of the current pulse. The second maximum of N_e coincides with the second maximum of the current pulse, i.e. with time position characterized by the most intense Be spectral lines around 12 μ s. As a conclusion, it can be said that optimal conditions for Be spectral line shapes measurements are achieved with $C = 5 \mu$ F, $U = 7$ kV, gas Ar +3% H $_2$, $p = 1.2$ mbar and that Be lines reach their maximum intensity at $t=12 \mu$ s.

3.4. Generation of dust particles

Throughout the course of the source construction and optimization of Be line shape measurements, significant quantity of the dust was produced. The appearance of the dust particles may be related to the existence of the second current maximum which is most likely to be a consequence of formation of negative ions that are the precursors of particle formation [36], see Fig. 2. Namely, the electron density, as shown in the Fig. 8, follows the current shape and this increase of the electron density after the main current pulse could be related to the charging and de-charging (ionization and recombination) of particles inside the plasma volume, as observed earlier in the pulsed complex plasma [36,37]. Anomalous behavior of the current pulse was used as a first sign that beryllium was ablated from the tube wall and that Be spectral line should appear in observed spectrum. Visible dust particles in the discharge were observed in the form of deposits on the observation window. These particles were noticed with gas flowing from the discharge tube support towards the output window. With the increase of discharge voltage, the generation of dust particles became more pronounced and appearance of the dust particles deposit on the observation window became clearly visible. After some time, the deposit covered window completely decreasing optical signal to that extent that further spectroscopic measurements were impossible. The interesting fact is that with subsequent current pulses two forms of the dust deposits were observed: cone shaped after odd and “half ring” shaped after even current pulse, see Fig. 9a and 9b, respectively, and the supplementary material in the form of movie. All measurements had to be taken in one hour and after

At this time the accumulated dust had to be removed and window had to be cleaned. To enable longer measurements the gas flow direction was reversed, meaning gas was flowing from the output window towards discharge tube support, see Sect. 3.3.1. In this configuration dust deposits were not observed, but the degradation of window still occurred, see Fig. 9c. This degradation of the window stopped occurring when special inlet at an angle of 45° angle with respect to discharge tube axis was installed, see Fig. 3c. This inlet did not prevent the degradation of the window when working with pressures less than 1 mbar and voltages higher than 7 kV.

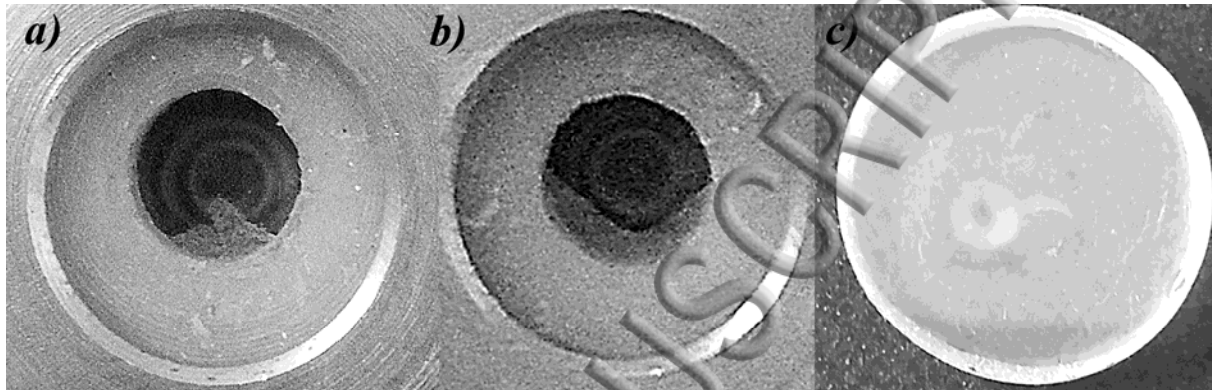


Figure 9. Two forms of dust deposits: a) cone, b) half-moon, c) degradation of the observation window caused by dust particles deposition.

Deposits on the observation window were easily cleaned and since the BeO is highly toxic, the dust particles were collected by exfoliation using adhesive tape, with all safety precautions, see Sect. 3.1. After that, tape was folded in order to insure dust particle isolation. When larger quantities of dust were collected from the discharge tube or from the liquid nitrogen trap, special handling and disposal procedure were performed. The dust particles were mixed with PMMA component in the glass bowl, after that the second component – resin was added and polymer with BeO dust was produced. In such a way, safe handling and disposal of toxic dust was enabled. For further precaution the glass bowl is closed with the lid, thus preventing possibility of evaporation if heated.

In order to study conditions for producing dust particles in the discharge, two additional tubes made from alumina and quartz were constructed, see description in Sec. 3.1. For both tubes dust particles were formed. Indication for dust formation was the appearance of the second current maximum, see Fig. 2b. Although occurrence and duration of the second current maximum, hence dust production, were slightly different for all three tubes, there were some common features: the dust was always formed when Ar was used as discharge gas; smaller retention of particles was observed for higher pressures; the deposition of particles on the observation window was more pronounced when working with low pressures and high voltages. However, two forms of dust deposits (cone shaped and “half ring”), that can be seen when working with BeO tube, were not noticed. Also, with SiO₂ tube dust was accumulated on the window even with reverse gas flow and with 45° angle inlet installed.

The study about influence of dust movements on spectral line shapes is in progress. Due to the high toxicity of dust, the shapes and dimensions of the obtained particles were not studied in this work.

CONCLUSIONS

In this work, the construction details and optimization of the low pressure pulsed discharge for safe beryllium spectra studies in the presence and in the absence of dust particles were presented. Beryllium lines were obtained from erosion of the discharge tube made of beryllium oxide ceramic, BeO. Electrical and spectroscopic studies were used for determination of the capacitance C , discharge voltage, gas type and pressure, as well as electrodes distance, diameter of electrode openings and other construction details. As a result, optimal conditions for beryllium lines observation are as follow: low inductance $5\ \mu\text{F}$ capacitor charged to $7\ \text{kV}$, $1.2\ \text{mbar}$ of $\text{Ar} + 3\% \text{H}_2$, $3\ \text{mm}$ diameter of the electrode opening and the smallest possible distance between electrodes and ceramic tube, see Fig. 3. and Sec. 3.3.2. At discharge voltages greater than $7\ \text{kV}$ the productions of dust particles became excessive, thus preventing study of the discharge tube material's particles on spectral line shapes. Using discharge tube modifications i.e. with gas inlet at 45° angle and reversed gas flow longer measurements were enabled.

Under the optimized conditions, studies of Be lines in the presence of the Be dust were enabled for the first time. From the point of signal to noise ratio, optimal emission spectra of Be was obtained from 10 to $20\ \mu\text{s}$ (measured from the beginning of the discharge), Fig. 2, coincident with the time of the second current maximum appearance. This shape of the current pulse was used as a first sign that beryllium was ablated from the tube wall and that Be spectral line should appear in observed spectrum. Stable operation of this novel beryllium plasma source creates the possibility of deepening the knowledge about the atomic data of Be, very much needed for the in situ examination of plasma facing materials in tokamak by LIBS.

Hypothesis of relation between the second current maximum and optimal spectral emission from the tube material was proved using two additional tubes made of SiO_2 and Al_2O_3 , even though discharge conditions differ. The dust particles were formed from all three tubes. In this way it is shown that this kind of low pressure pulsed discharge can be used for dust production and introduction of various materials into the plasma.

SUPPLEMENTARY MATERIAL

See supplementary material for the illustrations of two forms of dust deposits inside the discharge tube.

ACKNOWLEDGEMENT

This work has been financed by the Ministry of Education and Technological Development of the Republic of Serbia under the Project 171014. The authors thank Academician Prof. Emeritus Nikola Konjević for correcting manuscript and Stanko Milanović for technical assistance in preparation and setting up the experiment.

REFERENCES

- [1] G. Gilmore, B. Gustafsson, B. Edvardsson and P. E. Nissen, *Nature* 357, 379 (1992)
- [2] M. C. Galvez-Ortiz, E. Delgado-Mena, J. I. Gonzalez Hernandez, G. Israelian, N. C. Santos, R. Rebolo and A. Ecuivillon, *A&A* 530, A66 (2011)
- [3] N. Konjević and J. R. Roberts, *J. Phys. Chem. Ref. Data* 5, 209 (1976)
- [4] N. Konjević and W. L. Wiese, *J. Phys. Chem. Ref. Data* 5, 259 (1976)
- [5] N. Konjević, M. S. Dimitrijević and W. L. Wiese, *J. Phys. Chem. Ref. Data* 13, 619 (1984)
- [6] N. Konjević, M. S. Dimitrijević and W. L. Wiese, *J. Phys. Chem. Ref. Data* 13, 649 (1984)
- [7] N. Konjević and W. L. Wiese W, *J. Phys. Chem. Ref. Data* 19, 1307 (1990)
- [8] N. Konjević, A. Lesage, J. R. Fuhr and W. L. Wiese, *J. Phys. Chem. Ref. Data* 31, 819 (2002)
- [9] A. Lesage, *New Astronomy Reviews* 52, 471 (2009)
- [10] M. Platiša, J. Purić, N. Konjević and J. Labat, *Astronomy and Astrophysics* 15, 325 (1971)
- [11] J. Purić and N. Konjević, *Z. Phys.* 249, 440 (1972)
- [12] D. Hadžiomerspahić, M. Platiša, N. Konjević and M. Popović, *Z Phys.* 262, 169 (1973)
- [13] A. Sanchez, M. Blaha and W. W. Jones, *Phys. Rev. A* 8, 774 (1973)
- [14] H. P. Klug, *Review of Scientific Instruments* 12, 155 (1941)
- [15] H. Brackney and Z. J. Atlee, *Review of Scientific Instruments* 14, 59 (1943)
- [16] International Thermonuclear Fusion Experimental Reactor Project, ITER Report, ITER D 2X6K67 v1.0 Plant Description (PD), Cadarache (2009)
- [17] T. J. Dolan, *Magnetic Fusion Technology*, Springer, London (2013)

- [18] I. B. Kupriyanov, G. N. Nikolaev, L. A. Kurbatova, N. P. Porezanov, V. L. Podkovyrov, A. D. Muzichenko, A. M. Zhitlukhin, A. A. Gervash and V. M. Safronov, *Journal of Nuclear Materials* 463, 781 (2015)
- [19] G. R. Longhurst, L. L. Snead and A. A. Abou-Sena, *Proceedings of the Sixth International Workshop on Beryllium Technology for Fusion (Miyazaki, Japan)* 36, 2 (2004)
- [20] Z. Wang and C. M. Ticos, *Review of Scientific Instruments* 79, 10F333 (2008)
- [21] U. Kortshagen, *J. Phys. D: Appl. Phys.* 45, 253001 (2012)
- [22] P. K. Shukla and B. Eliasson, *Rev. Mod. Phys.* 81, 25 (2009)
- [23] G. E. Morfill and A. V. Ivlev, *Rev. Mod. Phys.* 81, 1353 (2009)
- [24] A. Piel A and A. Melzer, *Plasma Phys. Control. Fusion* 44, R1 (2002)
- [25] N. H. Brooks, A. Howald, K. Klepper and P. West, *Review of Scientific Instruments* 63, 5167 (1992)
- [26] R. J. Colchin, D. L. Hillis, R. Maingi, C. C. Klepper, and N. H. Brooks, *Review of Scientific Instruments* 74, 2068 (2003)
- [27] V. Morel, B. Pérès, A. Bultel, A. Hideur and C. Grisolia, *Phys. Scr.* 2016, 014016 (2016)
- [28] A. Semerok, D. L'Hermite, J. M. Weulersse, J. L. Lacour, G. Cheymol, M. Kempnaars, N. Bekris and C. Grisolia, *Spectrochimica Acta Part B* 123, 121 (2016)
- [29] <https://www-s.nist.gov/srmors/msds/1877-MSDS.pdf>
- [30] M. Ivković, T. Gajo, I. Savić and N. Konjević, *J. Quant. Spectrosc. Radiat. Transfer*, 161, 197 (2015)
- [31] T. Gajo, M. Ivković, N. Konjević, I. Savić, S. Djurović, Z. Mijatović and R. Kobilarov, *MNRAS* 455, 2969 (2016)

[32] M. Ivković, N. Konjević and Z. Pavlović, *J. Quant. Spectrosc. Radiat. Transfer* 154, 1 (2015)

[33] J. R. Fuhr and W. L. Wiese, *J. Phys. Chem. Ref. Data* 39, 013101 (2010)

[34] H. R. Griem, *Phys. Rev.* 131, 1170 (1963)

[35] L. Boufendi, J. Hermann, A. Bouchoule, B. Dubreuil, E. Stoffels, W. W. Stoffels and M. L. de Giorgi, *Journal of Applied Physics* 76, 148 (1994)

[36] J. Berndt, E. Kovačević, V. Selenin, I. Stefanović and J. Winter, *Plasma Sources Sci. Technol.* 15, 18 (2006)

[37] I. Stefanović, N. Sadeghi, J. Winter and B. Sikimić, *Plasma Sources Sci. Technol.* 26, 1 (2017)

ACCEPTED MANUSCRIPT

Forbidden component of the Be II 436.1 nm line recorded from pulsed gas discharge plasma

B. D. STANKOV^{1,2}, M. IVKOVIĆ^{1(a)}, M. VINIĆ¹ and N. KONJEVIĆ³

¹ *Institute of Physics, University of Belgrade - P.O.Box 68, 11080 Belgrade, Serbia*

² *University of Novi Sad, Faculty of Sciences, Department of Physics - Trg Dositeja Obradovića 4, 21000 Novi Sad, Serbia*

³ *Faculty of Physics, University of Belgrade - P.O.Box 368, 11000 Belgrade, Serbia*

received 27 June 2018; accepted in final form 13 September 2018

published online 10 October 2018

PACS 32.70.Jz – Line shapes, widths, and shifts

PACS 52.70.Kz – Optical (ultraviolet, visible, infrared) measurements

Abstract – We report results of the experimental study of the singly charged beryllium spectral line 436.1 nm, transition $3p^2P^{\circ}-4d^2D$, and forbidden component, transition $3p^2P-4f^2F^{\circ}$, which is for the first time identified in this work. Beryllium lines are recorded from gas discharge, after ablation of a beryllium oxide discharge tube, running in pulsed regime with the following gases: helium with traces of hydrogen, argon with traces of hydrogen and pure krypton. The ratio of line intensities and wavelength separation of the Be II 436.1 nm line and neighbouring line located at the blue wing are followed in the electron density range $(1.16-6.4) \times 10^{22} \text{ m}^{-3}$ determined from the hydrogen Balmer beta line (H_{β}) in the electron temperature interval between 10500 K and 15500 K. The functional dependence of the wavelength separation range and peak intensity ratio of these lines upon electron number density suggests the complex profile of the forbidden and allowed line, which can be used for diagnostics of low-temperature beryllium containing plasmas.

Copyright © EPLA, 2018

Introduction. – The subject of this experimental study is an investigation of the shape of the Be II 436.1 nm line which appeared with a strong component, located at the blue wing, in our gas discharge [1]. The assumption was that this may be the forbidden component of the allowed line 436.1 nm, and this work is an attempt to prove this hypothesis. If proven, this result will partially fill the gap between the investigations of this type of transitions along a lithium isoelectronic sequence, with already published data for Li I [2–4], C IV [5–7] and N V [7].

The spectral lines with forbidden components attracted attention some time ago, see, *e.g.*, [8], because of numerous applications in the field of Stark broadening theory testing, for electron number density, N_e , laboratory plasma diagnostics and in astrophysics for the analysis and modelling of the star atmosphere, see, *e.g.*, [9]. In addition, in the case of beryllium lines there are two more specific applications. One is related to the study of the inner plasma-wall interaction in ITER (International Thermonuclear Experimental Reactor) since this wall is considered to be covered with beryllium [10]. The other important field of

application is in astrophysics, considering that beryllium is a naturally occurring element in metal-poor stars [11].

Here, it should be emphasized that under a forbidden component (transitions with $\Delta l \neq \pm 1$, where l is the angular momentum quantum number) we consider lines which occur as a result of the breakdown of the parity selection rules induced by ambient plasma electric microfield. This effect has nothing to do with the forbiddenness associated to magnetic dipole, electric quadrupole or higher multipole transitions. A forbidden line starts to appear close to the allowed one when wave functions become mixed. It happens when plasma broadening of the allowed line becomes comparable with the energy levels separation between the allowed transition and the nearest dipole allowed perturbing level or levels. With an increase of the electric field (*i.e.*, an increase of the charged particles density), the mixing of the wave functions becomes stronger, and the wavelength difference between the allowed and forbidden components peaks becomes more pronounced. A further increment of the electric field brings an overall profile of the line shape close to the one of a hydrogen-like emitter with linear Stark effect. The conclusion here is that the overall shape of these lines is sensitive to the charged particle

^(a)E-mail: milivoje.ivkovic@ipb.ac.rs (corresponding author)

density. Therefore, it can be used for the N_e plasma diagnostics. It should be stressed that plasma conditions when a forbidden component becomes significant differ from element to element and even from line to line. The overall shape of lines with forbidden components to a smaller extent depends also on the electron temperature, reduced mass and ratio between electron and gas temperature [12], which opens possibilities for other plasma parameters diagnostics. The most frequently studied spectral lines of this type belong to the visible spectrum of He I, see, *e.g.*, [8,13,14]. The application of parameters of these lines for electron density diagnostics is demonstrated in several publications and references therein [12,15–21]. In addition, parameters of these lines are applied also for DC electric-field measurements, see, *e.g.*, [22,23].

To achieve the aim of this work, we recorded the overall shape of the Be II 436.1 nm line, together with nearby lines, in a discharge tube with different carrier gases. Simultaneously, N_e and the electron temperature, T_e and the dependence of the line profile parameters upon N_e were determined.

Experiment. – In this section the experimental setup, the measurement procedure as well as the method and results of plasma diagnostics will be described. The experimental apparatus was set up as for the standard end-on linear discharge plasma observation, see, *e.g.*, [1]. For data acquisition two spectra recording systems were used. In both cases the 1:1 axial image of the plasma source was projected onto the entrance slit of a monochromator, by the use of a focusing mirror and achromatic lens, see fig. 6 in [24]. Almost all spectral line shape recordings were performed using an imaging spectrometer (Shamrock 303 Andor), having instrumental half-width of 0.09 nm equipped with ICCD camera DH734 (Andor). These line shape recordings were performed with full vertical binning and gate width of 50 ns at various delay times. Delay times from the beginning of the current pulse, monitored by the Rogowski coil were determined with a digital delay generator (Stanford Research Systems, DG535). In order to check the influence of the instrumental broadening to the line shape, the cross-check with a second high-spectral-resolution recording system was performed. The spectra were obtained using a 1 m monochromator (McPherson Model 2051), having the instrumental half-width of 0.02 nm. This monochromator was supplied with a stepping motor and photomultiplier radiation detector, PMT (EMI 9658 R). The signal from the PMT was observed by the digital oscilloscope Tektronix TDS360 (bandwidth 200 MHz), triggered by the signal supplied from the Rogowski coil. The step motor rotates the diffraction grating of the monochromator so that, at different wavelengths, the radiation intensity can be recorded. The computer simultaneously collects data from the oscilloscope and controls the step motor. The end signal represents the mean value of 4 consecutive signals. This shot-to-shot technique was justified considering that the

pulse-to-pulse current reproducibility was better than 2%. More details about data acquisition and data manipulation can be found in [24].

Plasmas are created in a BeO ceramic discharge tube with inner diameter of 2.6 mm, outer diameter of 10 mm and length of 130 mm. Beryllium spectral lines are detected in the discharge after evaporation of Be off the inner tube wall by ablation induced by the discharge itself. Here, it should be emphasized that due to the toxicity of beryllium, a special procedure in handling the discharge tube and ablation products was always adapted [1]. The most important result of the previous study [1] is that the optimum conditions for excitation of Be spectral lines in our discharge are achieved when the capacitor $C = 5 \mu\text{F}$ is charged up to 7 kV in argon with 3% of hydrogen at $p = 1.2 \text{ mbar}$. At lower discharge voltages only lines of the carrier gas appear in spectra [1]. In addition, only at low gas pressure, $p < 5 \text{ mbar}$, the percentage of the beryllium atoms in the discharge becomes significant and Be becomes the main plasma constituent and most of the Be spectral lines appear in the recorded spectra.

In order to characterize the plasma source, diagnostics of N_e and T_e were performed. The electron number density, N_e , was determined from the peak separation $\Delta\lambda_{ps}$ of the H_β line using formula (6) from [25]:

$$\log N_e [\text{m}^{-3}] = A + B \log \Delta\lambda_{ps} [\text{nm}] = 22.65 + 1.53 \log \Delta\lambda_{ps} [\text{nm}]. \quad (1)$$

The values of parameters A and B are taken from [25] for a presupposed electron temperature of $13000 \pm 3000 \text{ K}$. For electron number densities determined in such a way, the electron temperature, T_e was estimated from the ratio of Be II 467.3 nm/Be I 457.3 line intensities using the formula

$$\frac{I_1}{I_2} = \frac{h^3}{2(2\pi mk)^{3/2}} \frac{(gA)_1 \lambda_1 N_e}{(gA)_2 \lambda_2 T_e^{3/2}} \times \exp\left(\frac{E_2 - E_1 + E_1^{ion} - \Delta E}{kT_e}\right). \quad (2)$$

After several iterations N_e and T_e were determined. The required transition probabilities were taken from the NIST database [26].

Since the Be lines have noticeable intensity in a very short time interval, the plasma diagnostics was performed only for times between $8 \mu\text{s}$ and $18 \mu\text{s}$ from the beginning of the current pulse. It should be stressed that N_e was determined only with a gas mixture of Ar with 3% H_2 , since the intensity of the H_β line under other experimental conditions was negligible. Namely, in the stated delay times interval, lines of other elements have very low intensity with the exception of O II lines (originating from the ablation products of BeO ceramics) and H_β . The recorded O II lines have a width equal to the instrumental width and they are located on the broad wings of the studied Be II line shape, see fig. 2, and, therefore, they are not convenient for N_e diagnostics. The intensity of H_β line

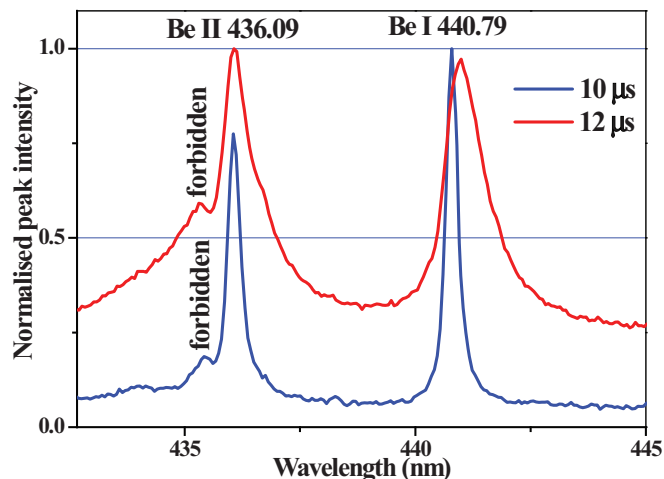


Fig. 1: (Colour online) Beryllium spectrum between 429 nm and 445 nm with normalised peak line intensities recorded in 1.2 mbar of He + 3% H₂ gas mixture at discharge voltage of 7 kV at different delays after beginning of the discharge current pulse.

at the time of interest in helium with 3% of hydrogen gas mixture was very weak and not usable for diagnostics as well. Small contribution of hydrogen traces in krypton plasma prevented detection of H_β line, also. The use of strong Be lines for N_e diagnostic has a significant drawback since their Stark widths may introduce inaccuracy due to pronounced self-absorption and even self-reversal in the case of resonant lines 313.0 nm and 313.1 nm.

Results and discussion. – The main result of this experimental study is the identification of the forbidden component $3p^2P-4f^2F^o$ along with allowed component $3p^2P^o-4d^2D$ of the Be II line at 436.1 nm in various gases. Although it has been previously stated [1] that the best conditions for excitation of beryllium lines were achieved when the carrier gas was argon, we first present the results in He with 3% H₂ plasma, see fig. 1. The reason for this being that in spectra recorded when the carrier gas was He with 3% H₂, only beryllium lines appeared, *e.g.*, there are no other lines that could entail confusion in the determination of a forbidden line shape and peak wavelength position.

However, in such discharge, beryllium lines appeared in a shorter period of time (10–12 μs). In order to confirm that the recorded line belongs to singly ionized beryllium and to analyse the possible influence of the Ar II and O II lines on the wavelength position and intensity of the forbidden component, spectra recordings were performed for Ar and Kr using the same discharge conditions that were employed for He with 3% H₂.

In fig. 2 recordings made from Ar plasma are presented. It can be seen that on the blue side of Be II 436.1 nm the appearance of other spectral lines can call into question the presence of the forbidden Be II line in the spectra presented in fig. 2. Lines which may interfere with the Be II 436.1 nm overall line profile belong to hydrogen Balmer

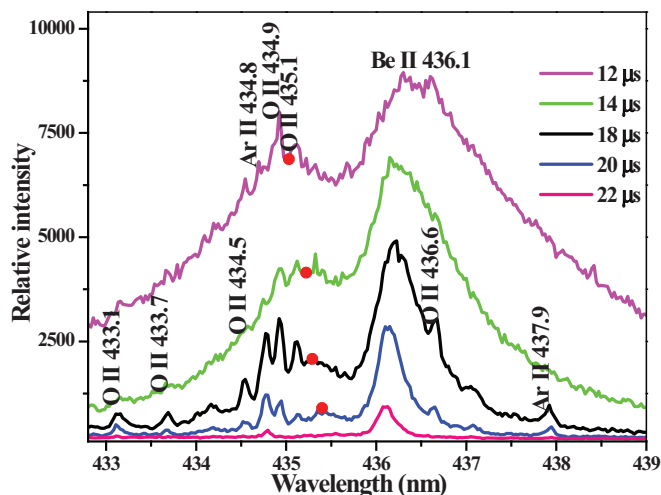


Fig. 2: (Colour online) Temporal evolution of the Be spectrum between 433 nm and 439 nm, recorded at discharge voltage of 7 kV at 1.2 mbar of Ar with 3% of H₂. The wavelength positions of the peaks are taken from [25]. Peak intensity and wavelength position of the forbidden component are denoted with circles and presented in table 1.

gamma (H_γ) 434.0 nm, Ar II at 434.81 nm and O II at 434.91 nm and 435.1 nm.

Having in mind the Stark shift and intensity of the H_γ, this line influence on the Be II 436.1 nm profile, at our experimental conditions, is small. Namely, for the estimated T_e of 10500 K–15500 K the H_γ line has at least twice lower peak intensity than the H_β line, recorded at the same experimental conditions, see fig. 5 in [1], and even smaller intensity at the position of the forbidden component due to the $\Delta\lambda^{-5/2}$ line wing dependence.

In order to resolve the influence of other non-hydrogenic plasma constituents, spectra recordings presented in fig. 2 were performed with smaller instrumental broadening, *i.e.*, the apparatus with better resolution, see section “Experiment”. From the results in fig. 2 one can conclude that the Ar II and O II lines may interfere in the determination of the peak wavelength position of the forbidden component. Fortunately, the difference in line widths (the forbidden line is much broader) confirms the existence of the forbidden component.

In the case of Kr plasma, fig. 3, the forbidden line is clearly visible, but its peak intensity and wavelength position are different in comparison with Ar plasma, under the same excitation conditions. Also, the appearance of the forbidden component in the Kr plasma is prolonged.

Differences between spectra recorded in various gases are illustrated by the change of ratio between the intensity of the allowed Be II line 436.1 nm and Be I line 440.79 nm, see figs. 1 and 3, thus indicating that the plasma parameters are incomparable.

In order to use the Be II line 436.1 nm with forbidden component $3p^2P-4f^2F^o$ for plasma diagnostics, the functional dependence of the wavelength separation between

Table 1: Temporal variation of N_e , T_e , s and F/A in argon with 3% of hydrogen for $p = 1.2$ mbar and $U = 7$ kV.

t (μ s)	N_e (10^{22} m $^{-3}$)	T_e (K)	s (nm)	F/A
10	6.40	15500	1.5	0.97
12	5.90	14200	1.3	0.78
14	5.00	13500	1.01	0.68
16	3.01	11980	0.93	0.55
18	1.16	10500	0.88	0.38
20			0.74	0.26

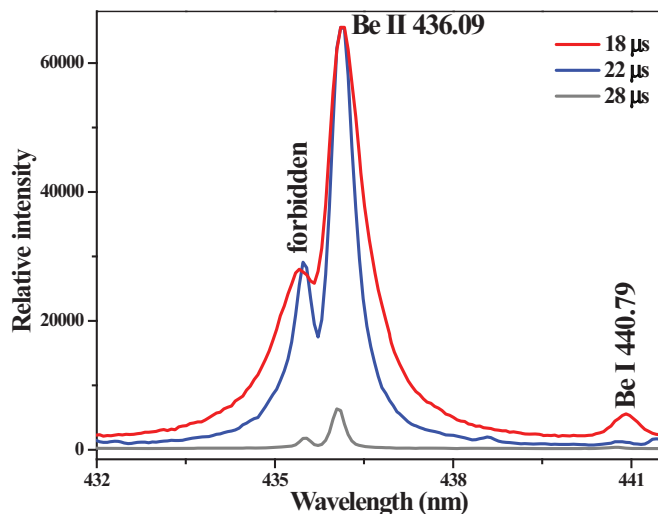
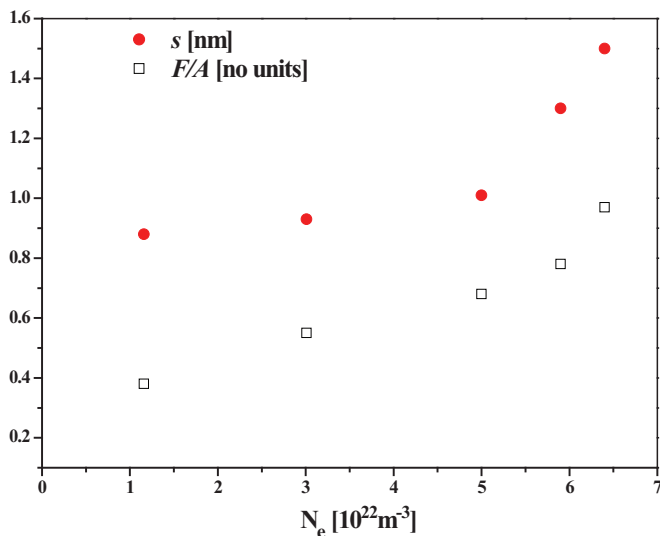


Fig. 3: (Colour online) Temporal evolution of the Be spectrum between 429 and 445 nm, recorded at discharge voltage of 7 kV at 1.2 mbar of Kr.

Fig. 4: (Colour online) The dependence of wavelength peaks separation s and peaks intensity ratio F/A dependence upon N_e for Be II allowed $3p^2P^{\circ}-4d^2D$ component and forbidden $3p^2P-4f^2F^{\circ}$ component at $p = 1.2$ mbar of Ar + 3% H $_2$ at $U = 7$ kV.

their peaks s , and/or the ratio between the maximum intensities of the forbidden component and allowed component, F/A , upon N_e should be determined. Unfortunately for our experimental conditions the Be II lines appear in a short time interval in which diagnostics of N_e is very difficult. Nevertheless, in spite of all the difficulties to determine the $s(N_e)$ and $F/A(N_e)$ dependences, we made an attempt to demonstrate the potential of this line with the forbidden component for the plasma diagnostics application, see fig. 4 and table 1.

The range of s and F/A and the corresponding N_e determined in the case of Ar with 3% H $_2$ suggests the possibility of using the Be II 436.1 nm line with forbidden component for plasma diagnostics purposes. Namely, it is shown that under our experimental conditions ($p = 1.2$ mbar, $U = 7$ kV and $C = 5$ μ F) during plasma generation and decay s changes between 0.74 nm and 1.5 nm, while F/A changes between 0.26 and 0.97 in the range of electron densities $(1.16-6.4) \times 10^{22}$ m $^{-3}$ and electron temperatures 10500 K–15500 K. The aforesaid functional dependence of wavelength separation and intensity ratios of two lines upon electron density are typical for lines with forbidden components. Unfortunately, a small N_e range does not allow the determination of the best-fit formulas $N_e = f(s)$ or $N_e = f(F/A)$ for reliable plasma diagnostics.

Conclusions. – On the bases of our experimental study we conclude that the spectral line located at the blue wing of the Be II 436.1 nm line, transition $3p^2P^{\circ}-4d^2D$, has all the characteristics of the forbidden transition. In order to prove that this line originates from the forbidden $3p^2P-4f^2F^{\circ}$ transition we carried out several studies like wavelength analysis of plasma impurities, measurement of the wavelength separation and ratios of two line intensities *vs.* electron number density. All results are indicating that the forbidden line $3p^2P-4f^2F^{\circ}$ is present in spectra of our discharge, which is well illustrated in figs. 1–3. The functional dependence of the wavelength separation and intensity ratios of two lines upon electron density are typical for lines with forbidden components, see, *e.g.*, He I lines [12,18–21]. Thus, on the basis of all the presented results one may conclude that the line at the blue wing of Be II 436.1 nm line, is a forbidden line belonging to the $3p^2P-4f^2F^{\circ}$ transition. Finally the wavelength separations and the ratios of peak line intensities in table 1 cannot be used for the testing of the overall line shape modelling of this beryllium allowed line with forbidden component since the influence of the allowed line optical thickness and additional electric field has not been examined in this work. For the same reason the data in table 1 may be applied for low-temperature plasma diagnostics with great precautions. One interesting application can be for the N_e determination during *in situ* examination of plasma facing materials in tokamak (containing beryllium) by laser-induced breakdown spectroscopy (LIBS) [27], in which electron density and temperature ranges are close to the values studied in this work.

On the basis of the analysis of energy levels along a lithium isoelectronic sequence for Li I [2–4], C IV [5–7], NV [7] and our results for Be II, we propose the study of the B III line 195.38 nm from the same transition $3p^2P^{\circ}-4d^2D$ in order to check whether the forbidden components, $3p^2P-4f^2F^{\circ}$ and $3p^2P-4f^2P^{\circ}$ will appear. In the present study of the Be II lines the forbidden component $3p^2P-4f^2P^{\circ}$ was not detected.

This work has been financed by the Ministry of Education and Technological Development of the Republic of Serbia under the Project 171014. The authors thank the technician STANKO MILANOVIĆ for technical assistance in the preparation and setting-up of the experiment.

REFERENCES

- [1] STANKOV B. D., VINIĆ M., GAVRILOVIĆ BOŽOVIĆ M. R. and IVKOVIĆ M., *Rev. Sci.*, **89** (2018) 053108.
- [2] JOVIĆEVIĆ S., GIGOSOS M. A., IVKOVIĆ M., GONZALEZ M. A. and KONJEVIĆ N., *Contributed Papers of the 22nd Summer School and International Symposium on the Physics of Ionized Gases (XXII SPIG, Kopaonik)* (Institute of Physics, Belgrade, Serbia) 2006, p. 315, ISBN 86-82441-18-7.
- [3] CVEJIĆ M., GAVRILOVIĆ M., JOVIĆEVIĆ S., IVKOVIĆ M. and KONJEVIĆ N., *EMSLIBS 2011 Euro Mediterranean Symposium on Laser Induced Breakdown Spectroscopy, Izmir, Turkey, 2011, Book of Abstracts* (Izmir Institute of Technology, Turkey) 2011, p. 128, <http://www.worldcat.org/title/euro-mediterranean-symposium-on-laser-induced-breakdown-spectroscopy-emslibs-2011-izmir-turkey-11-15-september-2011/oclc/75675399>.
- [4] CVEJIĆ M., STAMBULCHIK E., GAVRILOVIĆ M. R., JOVIĆEVIĆ S. and KONJEVIĆ N., *Spectrochim. Acta B*, **100** (2014) 86.
- [5] WERNER K., RAUCH T., HOYER D. and QUINET P., *Astrophys. J.*, **827** (2016) L4.
- [6] WERNER K., HOYER D., RAUCH T., KRUK J. W. and QUINET P., in *20th European White Dwarf Workshop*, edited by TREMBLAY P.-E., GÄNSICKE B. and MARSH T., *ASP Conference Series*, Vol. **509** (Astronomical Society of the Pacific) 2017.
- [7] BOTTCHE F., MUSIELOK J. and KUNZE H.-J., *Phys. Rev. A*, **36** (1987) 5.
- [8] GRIEM H. R., *Spectral Line Broadening by Plasmas* (Academic Press, New York) 1974.
- [9] BEAUCHAMP A., WESEMAEL F. and BERGERON P., *Astrophys. J. Suppl. Ser.*, **108** (1997) 559.
- [10] HOW J. and REICHLER R., International Thermonuclear Fusion Experimental Reactor Project 2009 ITER Report, ITER D 2X6K67 v1.0 Plant Description (PD) Cadarache.
- [11] GILMORE G., GUSTAFSSON B., EDVARDSSON B. and NIESSEN P. E., *Nature*, **357** (1992) 379.
- [12] GIGOSOS M. A. and GONZALEZ M. A., *Astron. Astrophys.*, **503** (2009) 293.
- [13] BEKEFI G., DEUTCH C. and YAAKOBI B., *Principles of Laser Plasmas* (John Wiley & Sons, New York) 1976.
- [14] CHERNICHOWSKI A. and CHAPPELLE J., *J. Quant. Spectrosc. Radiat. Transfer*, **33** (1985) 427.
- [15] UZELAC N. I. and KONJEVIĆ N., *Phys. Rev. A*, **33** (1986) 1349.
- [16] UZELAC N. I., STEFANOVIĆ I. and KONJEVIĆ N., *J. Quant. Spectrosc. Radiat. Transfer*, **46** (1991) 447.
- [17] PEREZ C., DE LA ROSA I., APARICIO J. A., MAR S. and GIGOSOS M. A., *Jpn. J. Appl. Phys.*, **35** (1996) 4073.
- [18] IVKOVIĆ M., JOVIĆEVIĆ S. and KONJEVIĆ N., *Spectrochim. Acta B*, **59** (2004) 591.
- [19] IVKOVIĆ M., GONZALEZ M. A., JOVIĆEVIĆ S., GIGOSOS M. A. and KONJEVIĆ N., *Spectrochim. Acta B*, **65** (2010) 234.
- [20] GONZALEZ M. A., IVKOVIĆ M., GIGOSOS M. A., JOVIĆEVIĆ S., LARA N. and KONJEVIĆ N., *J. Phys. D*, **44** (2011) 194010.
- [21] IVKOVIĆ M., GONZALEZ M. A., LARA N., GIGOSOS M. A. and KONJEVIĆ N., *J. Quant. Spectrosc. Radiat. Transfer*, **127** (2013) 82.
- [22] KURAICA M. M. and KONJEVIĆ N., *Appl. Phys. Lett.*, **70** (1997) 1521.
- [23] KURAICA M. M., KONJEVIĆ N. and VIDENOVIĆ I. R., *Spectrochim. Acta B*, **52** (1997) 45.
- [24] KONJEVIĆ N., IVKOVIĆ M. and SAKAN N., *Spectrochim. Acta B*, **76** (2012) 16.
- [25] IVKOVIĆ M., KONJEVIĆ N. and PAVLOVIĆ Z., *J. Quant. Spectrosc. Radiat. Transfer*, **154** (2015) 1.
- [26] https://physics.nist.gov/PhysRefData/ASD/lines_form.html.
- [27] MOREL V., PÉRÈS B., BULTELL A., HIDEUR A. and GRISOLIA C., *Phys. Scr.*, **T167** (2016) 014016.